From THE DEPARTMENT OF NEUROSCIENCE
Karolinska Institutet, Stockholm, Sweden

THE ROLE OF ABC TRANSPORTERS AND INFLAMMATION IN DRUG-RESISTANT EPILEPSY

Lora Deuitch Weidner

Stockholm 2017

Cover Art: Immunofluorescence image of a brain tissue sample from a patient with drug-resistant epilepsy. BCRP-positive capillaries are shown in green, neuronal COX-2 in red, and a nuclear counterstain in blue.

The Role of ABC Transporters and Inflammation in Drug-Resistant Epilepsy
THESIS FOR DOCTORAL DEGREE (Ph.D.)

By

Lora Deuitch Weidner

Principal Supervisor:
Dr. Jan Mulder
Karolinska Institutet
Department of Neuroscience

Co-supervisor(s):
Dr. Robert B. Innis
National Institutes of Health
National Institute of Mental Health

Dr. Matthew D. Hall
National Institutes of Health
National Center for Advancing Translational
Sciences

Professor Tomas Hökfelt
Karolinska Institutet
Department of Neuroscience

Opponent:
Professor Bjoern Bauer
University of Kentucky
Department of Pharmaceutical Sciences

Examination Board:
Professor Robert Harris
Karolinska Institutet
Department of Clinical Neuroscience

Professor Per Artursson
Uppsala Universitet
Department of Pharmacy

Professor Torbjörn Tomson
Karolinska Institutet
Department of Clinical Neuroscience

To my parents

Your unwavering dedication and commitment to my education has pushed me to be my best. I hope to always make you proud.

To my husband

It is because of your sacrifices that this work could come to fruition. Your love has seen me through the best and worst of times.

ABSTRACT

This thesis explores two pathologies thought to be related to drug resistance in epilepsy that may themselves be causally related: 1) overexpression of drug transporters in capillaries and 2) inflammation. With regard to the first hypothesis, overexpression of the ATP-binding cassette (ABC) transporters, P-glycoprotein (P-gp) and breast cancer resistance protein (BCRP), at the blood-brain barrier are thought to contribute to drug resistance in epilepsy. To measure ABC transporter activity in vivo, positron emission tomography (PET) imaging can be used, which requires a radiolabeled substrate and non-radiolabeled inhibitor. The second hypothesis suggests that inflammation increases P-gp expression and, conversely, that inhibiting inflammation decreases P-gp expression. Questions remain however, as to the interactions between ABC transporters and specific inflammatory proteins, as well as the cellular expression of the same inflammatory proteins in the human brain.

In **Paper I**, we characterized the BCRP inhibitor Ko143 to determine if it was a candidate for use in PET imaging. P-gp activity has been measured using PET imaging with tracers such as $[^{11}C]N$-*desmethyl*-loperamide (a P-gp substrate) along with a P-gp inhibitor such as tariquidar, but a similar imaging paradigm has not yet been developed for BCRP. Therefore, we performed multiple in vitro assays to characterize Ko143 and to measure its interaction with P-gp, BCRP, and the multidrug resistance transporter 1 (MRP1). Data from the in vitro assays indicated that while Ko143 was a potent BCRP inhibitor (IC_{50} = 9.7 nM), at higher concentrations it was a substrate for P-gp (IC_{50} = 2.7 μM) and MRP1.

In **Paper II**, because of reports questioning whether tariquidar is a P-gp inhibitor, we investigated tariquidar to determine the mechanism by which it interacts with P-gp. Using similar methods as outlined in Paper I, we found that tariquidar was a potent P-gp inhibitor at low concentrations (IC_{50} = 100 nM), but at higher micromolar concentrations it was a substrate and competitive inhibitor of BCRP.

In **Paper III**, we sought to determine whether a relationship exists between ABC transporter expression and expression of the inflammatory enzymes cyclooxygenase (COX)-1 and -2, as well as the inflammation biomarker, translocator protein 18 kDa (TSPO). We used multiplex immunofluorescence to measure the expression of P-gp and BCRP as well as COX-1, COX-2, and TSPO in brain tissue samples from people with drug-resistant epilepsy. These tissue samples were classified as either having mesial temporal sclerosis (MTS) or not (non-MTS), in which the non-MTS samples acted as control tissue for MTS samples. When investigating the relationship between ABC transporters and the inflammatory proteins, the only correlation we observed was between BCRP and TSPO, in which increased BCRP density correlated linearly with increased TSPO density (P = 0.0003, r = 0.72131). No significant differences were found in the expression of any protein measured between MTS and non-MTS tissue samples.

In **Paper IV**, we investigated the cellular expression of three inflammatory proteins COX-1, COX-2, and TSPO in brain tissue samples from people with drug-resistant epilepsy. To do so, we used multiplex immunofluorescence microscopy to measure the expression of these proteins in microglia, astrocytes, and neurons. We found that that COX-1 was predominately expressed in microglia, while COX-2 and TSPO were expressed in microglia and neurons.

In summary, this thesis explored the mechanisms underlying drug resistance in epilepsy. We studied overexpression of ABC transporters and inflammation, two pathologies hypothesized to be involved in drug-resistant epilepsy that may themselves possibly be related. While Ko143 is specific for BCRP at nanomolar concentrations (similar to tariquidar for P-gp), its potential utility as a radiolabeled inhibitor was diminished by the fact that PET requires picomolar affinity—rather than the 9.7 nM we measured—to measure the low density of BCRP in the brain. With regard to inflammation, we found that COX-1 is primarily expressed in microglia, a trait that makes it, rather than COX-2, a better radioligand for studying neuroinflammation in patients with drug-resistant epilepsy, given that microglia produce the majority of pro-inflammatory cytokines in the brain.

LIST OF THESIS PUBLICATIONS

I. **The inhibitor Ko143 is not specific for ABCG2**. Weidner LD, Zoghbi SS, Lu S, Shukla S, Ambudkar SV, Pike VW, Mulder J, Gottesman MM, Innis RB, Hall MD. *J. Pharmacol. Exp. Ther.* 2015 Sep;354(3):384-93

II. **Tariquidar is an inhibitor and not a substrate of human and mouse P-glycoprotein**. Weidner LD*, Fung KL*, Kannan P, Moen JK, Kumar JS, Mulder J, Innis RB, Gottesman MM, Hall MD. *Drug Metab. Dispos.* 2016 Feb;44(2):275-82
* = authors contributed equally

III. **The influence of tissue pathology and inflammation on the density of two efflux transporters in drug-resistant mesial temporal lobe epilepsy**. Weidner LD, Theodore WH, Kannan P, Mitsios N, Kang SJ, Hall MD, Innis RB, Mulder J.

Manuscript

IV. **Expression of cyclooxygenase-1 and -2 in mesial temporal lobe resected from patients with drug-resistant epilepsy**. Weidner LD, Kannan P, Mitsios N, Kang SJ, Theodore WH, Hall MD, Innis RB, Mulder J.

Manuscript

LIST OF NON-THESIS PUBLICATIONS

I. **An automated method measures variability in P-glycoprotein and ABCG2 densities across brain regions and brain matter**. Kannan P, Schain M*, Kretzschmar WW*, Weidner LD*, Mitsios N, Gulyás B, Blom H, Gottesman MM, Innis RB, Hall MD, Mulder J. *J. Cereb. Blood Flow Metab.* 2017 Jun;37(6):2062-2075
* = authors contributed equally

CONTENTS

LIST OF ABBREVIATIONS

ABC	ATP-binding cassette
ABCB1	Human gene that encodes for P-gp
ABCG2	Human gene that encodes for BCRP
AED	Antiepileptic drug
ATP	Adenosine triphosphate
BBB	Blood-brain barrier
BCRP	Breast cancer resistance protein
COX	Cyclooxygenase
dLop	*N-desmethyl*-loperamide
HRP	Horseradish peroxidase
LPS	Lipopolysaccharide
Mdr1a/1b	Mouse genes that encodes for P-gp
MRP1	Multidrug resistance protein 1
MTS	Mesial temporal sclerosis
PBS	Phosphate-buffered saline
PET	Positron emission tomography
P-gp	P-glycoprotein
ROI	Region of interest
TSPO	Translocator protein 18 kDa

1 INTRODUCTION

1.1 ABC TRANSPORTERS

Treating a disease is a difficult task given the number of factors that have to be considered to ensure the therapy is effective. Treatment is further complicated if resistance develops to the medication, reducing treatment efficacy and patient quality-of-life. One mechanism of resistance involves reduction in cellular or tissue accumulation of therapeutics by the adenosine triphosphate (ATP) binding cassette (ABC) transporters. ABC transporters are endogenous efflux pumps that serve to protect cells from xenobiotics, and are strategically positioned in many blood-tissue (or blood-tumor) barriers throughout the body [1]. Overexpression of these transporters reduces the amount of drug that can diffuse into the tissue, thus conferring resistance in diseases such as cancer, human immunodeficiency virus (HIV), and epilepsy [2, 3]. As a consequence of reduced drug penetration, higher doses of medication are needed to maintain therapeutic effects, which can subsequently increase the risk for toxicity [4].

The blood-brain barrier (BBB) poses a particularly difficult drug delivery hurdle to overcome when treating neurological diseases. The non-fenestrated blood vessels (capillaries) that comprise the BBB prevent paracellular entry to the brain (Figure 1) [5]. To cross the BBB, molecules need to have a low molecular weight (< 400 Da) and be highly lipid soluble in order to diffuse across brain endothelial cells [6]. To facilitate passage of biologically essential hydrophilic molecules that do not fit these parameters, carrier-mediated influx pumps such as glucose transporter 1 and organic anion transporter 2 exist to transport glucose and organic ions, respectively [7, 8]. Most drug-like molecules with the molecular properties to passively diffuse across the membranes of endothelial cells are often effluxed back into the lumen by ABC transporters [9]. The human genome encodes 48 members of the ABC family, eight of which are transporters expressed in the BBB [10]. Of these, P-glycoprotein (P-gp) and breast cancer resistance protein (BCRP) are the two transporters most extensively studied (Figure 1).

1.1.1 P-glycoprotein (P-gp)

P-gp (also called ABCB1 or MDR1) is a 170 kDa glycoprotein encoded by the *ABCB1* gene, and was first identified in colchicine-resistant Chinese hamster ovary cells [11, 12]. It is made up of two structurally identical regions, each containing a membrane-spanning region and a nucleotide-binding domain, which are joined by a linker [13]. Expression of P-gp is highest in tissues that have an excretory function such as the intestine, liver, and kidneys, as well as in tissues requiring extra protection such as the blood-placenta and BBB [14]. P-gp functions by recognizing substrates in the lipid membrane and utilizing an ATP to pump the molecule against its concentration gradient back into the lumen [15, 16]. Substrates of P-gp include a wide range of xenobiotics such as antiepileptic drugs (AEDs), immunosuppresors, HIV protease inhibitors, and analgesics [14]. P-gp can also recognize some endogenous compounds of varying size such as beta amyloid, steroids, lipids, and small cytokines [14, 17].
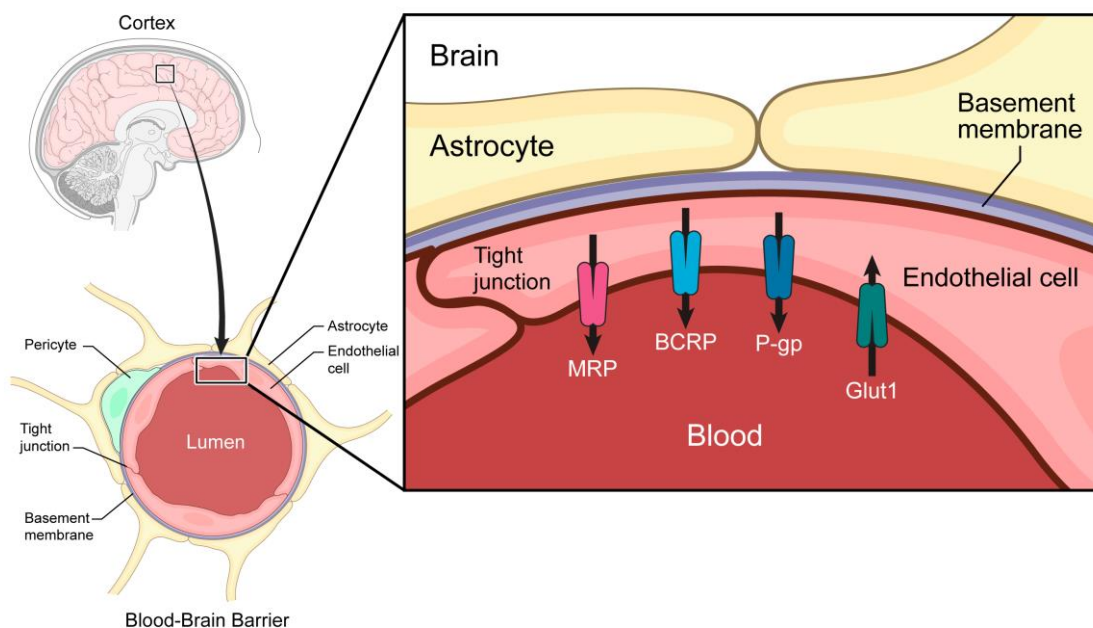
Figure 1. Representation of ATP binding cassette (ABC) transporters present in the blood-brain barrier (BBB). The BBB is comprised of endothelial cells with tight junctions to protect the brain from potentially harmful molecules in the blood. Molecules necessary for brain function, such as glucose, bypass the BBB via influx transporters, such as glucose transporter 1 (Glut1). P-glycoprotein (P-gp), breast cancer resistance protein (BCRP), and multidrug resistance protein (MRP) are ABC transporters that are responsible for effluxing xenobiotics from the brain into the blood.

1.1.2 Breast cancer resistance protein (BCRP)

BCRP (also called ABCG2 or MXR) is encoded by the *ABCG2* gene and was first discovered in a multidrug-resistant breast cancer cell line (which is how it got its name) [18]. Its structure differs from P-gp in that BCRP is a homodimer made up of two 'half-transporters'. Each half is 72 kDa and contains a transmembrane domain and an ATP-binding domain that need to dimerize to form a functional transporter unit [19]. Despite the difference in structure, BCRP performs the same function as P-gp and recognizes many of the same substrates, although chemotherapeutics like mitoxantrone are thought to be specific BCRP substrates [20]. BCRP is generally co-expressed in the same blood-tissue barriers as P-gp, and is also highly expressed in the canonical 'side-population' of cancer stem cells (for review see [21]). Certain polymorphisms of BCRP result in reduced function or non-functional variants, and while the former has some impact on substrate recognition, the latter increases the risk of hyperuricemia and gout [22, 23].

1.1.3 Inhibitors of P-gp and BCRP

The ability of P-gp and BCRP to recognize a wide array of substrates complicates drug delivery to the brain. Because of this, inhibitors have been developed to circumvent the efflux action of ABC transporters, initially with the intention of addressing transporter-mediated multidrug resistance in cancer. Three generations of P-gp inhibitors have been tested in vitro, in vivo, and
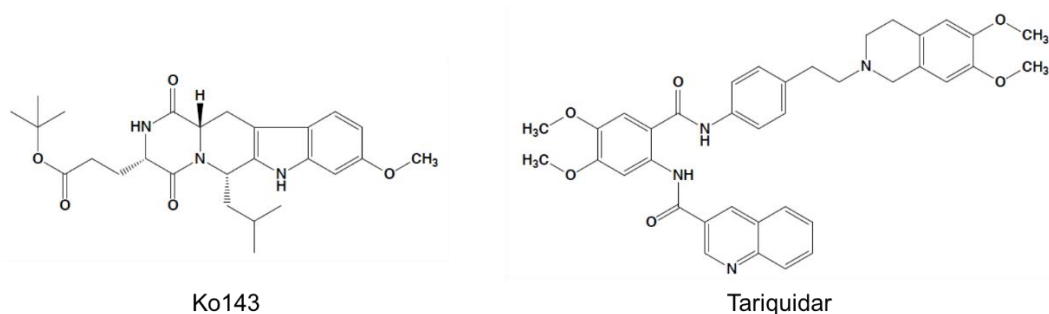
2

Figure 2. Chemical structures of a BCRP inhibitor (Ko143) and a P-gp inhibitor (tariquidar).

in clinical trials, but while some of these inhibitors are quite effective in vitro, the clinical data has failed to mirror this success [24, 25]. Of the third-generation inhibitors, tariquidar is the most potent P-gp inhibitor (Figure 2) [26]. When tested in cancer clinical trials, tariquidar was found to be ineffective at improving response to chemotherapy, and displayed moderate toxicity, presumably from 'on-target' inhibitory effects on P-gp in the liver, kidney, and at other sites [27]. Despite the negative results, tariquidar is frequently used as a tool in vitro and in animal models to study the activity of P-gp. At higher concentrations, tariquidar is a substrate of BCRP, but is a specific P-gp inhibitor at nanomolar concentrations [28]. Several potent inhibitors for BCRP have been utilized in vitro and in animal studies, such as fumitremorgin C (which cannot be used in vivo due to neurotoxicity) and its non-toxic analogue Ko143 (Figure 2), however to date none have been employed in a clinical trial [20, 29].

1.1.4 Imaging P-gp and BCRP

Imaging ABC transporters with positron emission tomography (PET) is the only non-invasive way to measure the activity or density of transporters in humans in vivo. Knowing the pathological role ABC transporters play could benefit the development of drugs able to cross the BBB. In order to measure P-gp or BCRP activity with PET, a drug (substrate) that is recognized by P-gp or BRCP, and is amenable to radiolabeling, is required. At baseline, a substrate radiotracer will not be able to enter the brain due to its efflux by P-gp or BCRP (or both). This is why an inhibitor (not radiolabeled) is needed at pharmacologic doses to block the efflux action of P-gp or BCRP. Accumulation of the substrate radiotracer in the brain after inhibition can then be measured. However, developing a substrate radiotracer for a specific ABC transporter is a challenge given the overlapping ligand affinity between P-gp and BCRP, and is made even more complicated because of the stringent requirements for a suitable PET radiotracer [30, 31].

1.1.4.1 P-gp

For P-gp, there are several successful radiotracers that can be used to measure both activity or density. Radiotracers for measuring P-gp activity include the single photon emission computed tomography tracer [99mTc]sestamibi, as well as the PET tracers [11C]verapamil and [11C]*N-desmethyl*-loperamide ([11C]dLop) [32-34]. Although [99mTc]sestamibi has been used
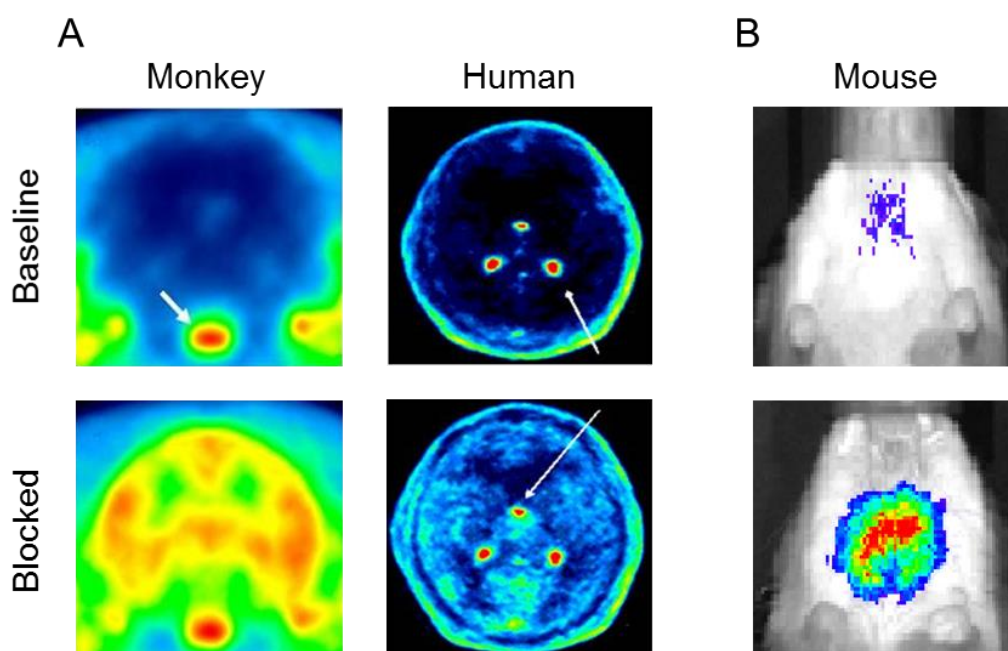
Figure 3. Imaging ABC transporters in vivo. (A) PET images of [^{11}C]*N-desmethyl*-loperamide (dLop), a P-gp substrate radiotracer, in monkey and human brains. At baseline (top) there is no brain signal, and inhibition of P-gp with an inhibitor (bottom) is necessary for uptake of [^{11}C]dLop into the brain. (B) Bioluminescent signal due to uptake of D-luciferin into the mouse brain before (top) and after administration of 10 mg/kg Ko143 (bottom). Because D-luciferin is a substrate of the ABC transporter BCRP, inhibition of BCRP with Ko143 is necessary for uptake of D-luciferin into the brain.

in the clinic more than any other P-gp radiotracer (for tumor imaging), [^{99m}Tc]sestamibi is also a substrate of BCRP and two other ABC transporters, multidrug resistance protein (MRP)-1 and -2 [35], making it a poor candidate to specifically measure P-gp activity at the BBB. At micromolar concentrations verapamil acts as an inhibitor of P-gp, but at the picomolar concentrations used in PET, it behaves as a substrate and can therefore be used to measure P-gp activity [15]. [^{11}C]dLop is considered a better radiotracer than [^{11}C]verapamil because it has a stronger affinity for P-gp (as evident by lower baseline signal), and is trapped in lysosomes which boosts brain signal (Figure 3A) [33]. Non-radiolabeled tariquidar is often used as the P-gp inhibitor during scans with [^{11}C]verapamil or [^{11}C]dLop, and has been administered in humans at a dose of 2-6 mg/kg (though these doses do not fully inhibit P-gp) (Figure 3A) [36].

To measure P-gp density, radiolabeled inhibitors such as [^{11}C]elacridar, [^{11}C]tariquidar, and [^{11}C]laniquidar have been explored [37]. As inhibitors, these radiotracers are not transported by P-gp like [^{11}C]dLop, but instead bind directly to P-gp (though this has been considered controversial, and is addressed in this thesis) [31]. Although the density of P-gp is high within the capillary bed itself (40 nM), its concentration per cm^3 of tissue (which PET measures) is quite low (estimated to be 1.3 nM) due to the relatively low percentage of endothelial cells within the whole brain. This low density in tissue as a whole would require a radioligand with picomolar affinity, which is not the case for the aforementioned radiotracers [31].

1.1.4.2 BCRP

There are currently no successful BCRP substrate radiotracers for use in PET. Attempts to label BCRP substrates have been reported but none have been implemented in humans [38]. Dantrolene, a muscle relaxant and a possible BCRP-specific substrate, was radiolabeled for imaging studies in rodents but no imaging results have been published thus far [39, 40]. Imaging studies were performed with [^{11}C]befloxatone in rats, and while befloxatone is a BCRP substrate in vitro, its uptake in vivo was not affected by BCRP [41].

In mice however, there are two methods to measure BCRP activity. The first involves measuring the uptake of [^{11}C]tariquidar (a substrate of BCRP) in a P-gp knockout mouse before and after inhibition of BCRP with Ko143 [42]. By genetically knocking out P-gp, any change in uptake of [^{11}C]tariquidar can be solely attributed to BCRP. The second method involves measuring bioluminescence in the brain of transgenic mice (Figure 3B) [43]. These mice express firefly luciferase (fLuc) in astrocytes behind the BBB, and when they are injected with the fLuc substrate D-luciferin, bioluminescence is produced in the brain. Because D-luciferin is a BCRP substrate, co-administration of Ko143, or another BCRP inhibitor, is required to elevate the bioluminescent signal (Figure 3B) [43]. Neither of these methods however, can be applied to humans, so the search for a suitable BCRP substrate radiotracer remains ongoing.

1.2 EPILEPSY

Drug resistance affects approximately 30 percent of all persons diagnosed with epilepsy. Drug-resistant epilepsy is defined as "a failure of adequate trials of two (or more) tolerated… AED regimens… to achieve freedom from seizures" [44]. For patients with drug-resistant epilepsy, the most effective treatment is often the surgical resection of the epileptic focus [45]. Several hypotheses exist to explain why these patients are unresponsive to AEDs, the two most prevalent being the "target hypothesis" and the "transporter hypothesis" [44]. The target hypothesis states that the intended drug targets themselves have changed, so that the drug can no longer bind to its receptor and exert an effect. Although there has been some research that supports this notion, this does not explain why drug-resistant patients are non-responsive to drugs with different mechanisms of action [44].

1.2.1 The transporter hypothesis

The transporter hypothesis proposes that ABC transporters are responsible for preventing entry of AEDs into the brain (Figure 4) [44]. The validity of this hypothesis relies on research showing an upregulation of ABC transporter expression or function in the brain capillaries of patients with drug-resistant epilepsy. Multiple groups have investigated the expression of P-gp in brain tissue samples from patients with drug-resistant epilepsy, and have found a consistent increase in expression when compared to control tissue. These studies were conducted using tissue samples from patients with some form of temporal lobe epilepsy [46-52], focal cortical dysplasia [51, 53, 54], tuberous sclerosis [55], or brain tumor [51, 54]. A potential caveat of these studies is the type of control tissue used as a comparison. Since it is impossible to obtain
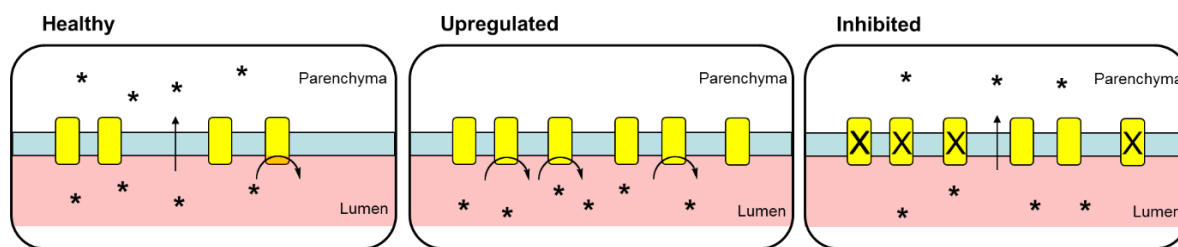
Figure 4. Diagram of the transporter hypothesis of drug-resistant epilepsy. ABC transporters (yellow squares) are endogenously expressed in the healthy brain at normal levels (left panel), which permits passage of xenobiotics like antiepileptic drugs (AEDs, asterisks) into the brain. In drug-resistant epilepsy (center panel), ABC transporter expression is upregulated and therefore prevents passage of AEDs into the brain. To bypass the efflux mechanism of the ABC transporters, transporter-specific inhibitors (X's) can be administered (right panel), allowing AEDs to enter the brain.

surgically resected tissue from healthy people, these studies had to rely on postmortem samples, tissue obtained through other types of brain surgery, or commercially purchased cell cultures. A lack of available proper control tissue makes these findings difficult to interpret and less conclusive. It is not clear if ABC transporters are also overexpressed in healthy people, or in patients with drug-responsive epilepsy.

For BCRP, there are mixed results as to whether expression is increased in drug-resistant epilepsy. No upregulation of BCRP was detected in samples with hippocampal sclerosis, focal cortical dysplasia, or dysembroplastic neuroepithelial tumor [56]. And while a second study also found no upregulation of BCRP in hippocampal sclerosis tissue samples, they did find an upregulation of BCRP in tissue from brain tumors associated with epilepsy pathologies [57]. In capillaries isolated from pediatric patients with drug-resistant epilepsy, BCRP expression decreased after the addition of glutamate, which is the opposite of what is expected given that P-gp expression increased using the same model [58].

In addition to increased ABC transporter expression, in order for the transporter hypothesis to be upheld, ABC transporters need to recognize AEDs as substrates. In other words, if AEDs are not substrates of drug efflux transporters, then the overexpression of ABC transporters should have no impact on AED efficacy. There have been numerous studies conducted investigating whether ABC transporters recognize commonly used AEDs. For P-gp, there is in vitro and in vivo evidence that AEDs such as phenytoin and phenobarbital are weak substrates [59], while for BCRP the results are conflicting [60, 61]. Based on this, the P-gp inhibitor verapamil has been investigated as an adjuvant therapy for patients with drug-resistant epilepsy. While some studies reported a positive influence of verapamil in addition to AEDs [62-64], a double-blinded, placebo-controlled trial found the addition of verapamil to have only a mild benefit [65].

1.2.2 Imaging P-gp activity in epilepsy

P-gp radiotracers have been used in rodent seizure models as well as in humans to explore whether P-gp activity or density are increased in drug-resistant epilepsy. In a rat model of temporal lobe epilepsy, those animals deemed 'non-responders' (drug-resistant) showed a significant increase of [^{18}F]MPPF (a P-gp substrate radiotracer) activity in the brain after tariquidar treatment as compared to the 'responder' group [66]. However in another study, only small changes were detected in the baseline uptake of [^{11}C]verapamil in kainate seizure-induced rats versus controls, in which inhibition via tariquidar increased brain uptake equally in both groups [67]. No difference in brain signal before and after tariquidar dosing was observed in electrode-implanted rats using [^{11}C]quinidine (a P-gp inhibitor radiotracer) and [^{11}C]laniquidar [68]. The first application of [^{11}C]verapamil in patients with drug-resistant epilepsy showed no statistically significant differences in uptake between epileptogenic and nonepileptogenic brain regions [69]. However, a follow up study with a larger patient cohort did reveal decreased [^{11}C]verapamil uptake in drug-resistant epileptics than in seizure free patients in certain temporal lobe regions. In addition, administration of tariquidar resulted in less uptake of [^{11}C]verapamil in drug-resistant patients compared to healthy controls [70]. Both of these responses (i.e., decreased uptake of verapamil before and after tariquidar) are consistent with drug-resistance being associated with, and perhaps caused by, increased activity of P-gp.

1.3 INFLAMMATION

1.3.1 ABC transporters and inflammation

A different approach to inhibiting ABC transporter efflux is to understand the pathways that regulate transporter expression. Understanding these mechanisms could reveal upstream targets that could be manipulated to decrease transporter activity or expression. One of these processes is thought to be inflammation [71]. Studies conducted within the past decade have found a strong connection between inflammation and P-gp expression. Increases in inflammatory markers have been measured in brain tissue from patients with epilepsy with an autoimmune or viral origin, but the involvement of inflammation in mesial temporal lobe epilepsy is unknown [72]. It is also unknown whether inflammation is merely a byproduct of seizure activity or a contributing factor to the progression of the disease [72]. Nonetheless, modulation of P-gp expression through pharmacologic manipulation of specific inflammatory markers is a possible method to increase drug delivery to the brain.

The link between P-gp expression and inflammation was first studied in the intestine and the liver. There are mixed data regarding the expression of P-gp in models of intestinal inflammation. In tissue samples from patients with active ulcerative colitis [73, 74], Crohn's disease, collagenous colitis, and diverticulitis patients [73], P-gp expression was downregulated compared to control tissue. In an induced inflammation model in rats, P-gp expression was decreased in the inflamed tissue [75, 76], but increased in the surrounding healthy tissue, suggesting a compensatory mechanism [75]. The same decrease in P-gp

expression was also observed in a lipopolysaccharide (LPS) model of inflammation in rats [77]. On the other hand, increases in P-gp expression were measured in human tissue samples of ulcerative colitis [78]. In biopsies from children with Crohn's disease, P-gp mRNA levels were significantly higher than in control tissue [79]. Tissue from an experimental rat colitis model displayed a slight increase in P-gp activity [80]. Exposure of Caco-2 cells (a model of intestinal P-gp) to pro-inflammatory cytokines through direct addition or by co-culturing with macrophages increased P-gp mRNA expression [81]. In rats, indomethacin-induced small intestinal ulcerations and adjuvant-induced arthritis did not have any effect on *mdr1a* mRNA expression [82], and *mdr1a/1b* mRNA expression [83], respectively.

For hepatic P-gp, there seems to be a consistent outcome of decreased expression during inflammation. In models of induced inflammation, P-gp expression decreased after administration of the LPS [84-88], turpentine [85, 87, 89], interleukin (IL)-6 [85, 89-92], IL-1β [91, 92], tumor necrosis factor alpha (TNFα) [91], and in an adjuvant-induced model of arthritis [83]. In a follow up study however, IL-1β and TNFα were found to increase *mdr1b* mRNA [85]. Additionally, *MDR1* mRNA expression was the same in tissue from patients with inflammation-induced icteric cholestasis as compared to controls [93]. This discrepancy in outcome for both intestinal and hepatic P-gp expression may be due to the model used. Fernandez and colleagues found that P-gp expression differs depending on what compound is used to induce inflammation, but nevertheless concluded that there is a general trend of decreased P-gp expression and function in the intestine and liver [94].

Similar to the liver and intestine, changes in P-gp expression at the BBB seem to be dependent in part on the model used to study inflammation. Increases in P-gp have been observed after exposure to lymphocytes [95], 6-hydroxydopamine [96], TNFα [97-101], IL-1β [99], endothelin 1 [97, 102], and diesel exhaust particles [103]. Conversely, decreases have been observed after exposure to LPS [84, 88, 104], IL-6 [98, 99], HIV-1 viral envelope glycoprotein [99], and IL-1β [100]. Bauer and colleagues found that the time-course for their experiments dictated the type of P-gp modulation, reinforcing the importance of study design. In isolated rat brain capillaries, initial administration of either TNFα or endothelin 1 acutely decreased P-gp expression, which then rebounded and doubled that of control capillaries after six hours [97]. For BCRP, TNFα, IL-1β [100], and LPS injection [104] decreased expression while endothelin 1 increased expression [102].

1.3.2 Translocator protein

Originally called the peripheral benzodiazepine receptor, translocator protein 18 kDa (TSPO) is a transporter located in the outer mitochondrial membrane. TSPO is thought to transport cholesterol to an enzyme which converts it to pregnenolone, a precursor for steroids and neurosteroids [105]. TSPO is highly expressed in microglia and astrocytes; increases of TSPO correlate to increases in microglia activity, therefore making TSPO a biomarker of inflammation [106]. Increases in TSPO expression is also observed in diseases such as epilepsy, Alzheimer's disease, and Parkinson's disease [105, 107, 108].

To measure TSPO activity in the brain, the radiotracers [^{11}C]PK11195, [^{11}C]PBR28, and [^{11}C]DPA-713 have been developed. In rat models of temporal lobe epilepsy, increases in [^{11}C]DPA-713 signal correlated with symptom severity [109], and with brain areas known to be affected by kainic acid [110]. One study measuring neuroinflammation in a rat model of drug-resistant epilepsy found increased TSPO signal (using [^{11}C]PK11195) in rats considered to be 'non-responders' to AEDs compared to 'responders' and non-epileptic controls. The authors could not definitively conclude that this was related to drug resistance however, because the 'non-responders' also exhibited higher seizure severity [111]. In humans, there was an increase in [^{11}C]PBR28 and [^{11}C]DPA-713 signal ipsilateral to the seizure focus compared to the contralateral side, as well as compared to age-matched healthy controls [106, 112].

1.3.3 Cyclooxygenase

Cyclooxygenases (COX) are enzymes involved in the inflammatory cascade, and act by converting arachidonic acid into prostanoids (Figure 5) [113]. The two isoforms COX-1 and COX-2 are thought to hold opposing roles during an inflammatory response. COX-1 is understood as being responsible for homeostatic prostaglandin synthesis, while COX-2 is thought to be a pro-inflammatory marker, in which expression is acutely increased after an inflammatory event [114]. However recent studies have challenged these notions by showing that COX-1 also has a pro-inflammatory role, and that COX-2 can have anti-inflammatory functions [115]. COX-1 and COX-2 also differ in cellular expression in the brain. Both are expressed in microglia and endothelial cells, but COX-1 is also found in macrophages, while COX-2 is also expressed in neurons [114, 115].

When expression of COX-2 was shown to be upregulated in tumors, studies began to investigate possible links between COX-2 and ABC transporters. In breast [116] and ovarian [117, 118] cancer tissue samples, increases in COX-2 expression correlated with increases in
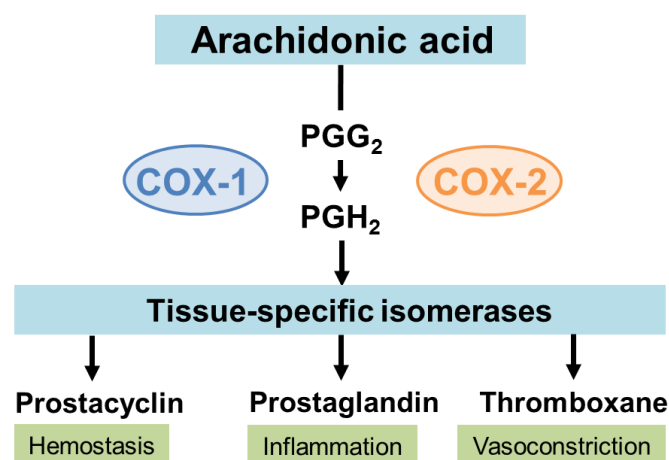

Figure 5. Flow chart of the cyclooxygenase (COX) cascade. Both COX-1 and COX-2 work by converting arachidonic acid into prostaglandin G$_2$ (PGG$_2$) and then into prostaglandin H$_2$ (PGH$_2$). PGH$_2$ is then converted into one of three types of prostanoids: prostacyclin, prostaglandin, or thromboxane.

P-gp expression. P-gp expression increased after transfecting rat mesangial cells with COX-2 [119], after the addition of prostaglandin E2 to primary rat hepatocyte cultures [120], and by exposing caco-2 cells to trinitrobeneze sulfonic acid [121]. The latter was also reproduced in vivo [121]. Cell lines expressing high levels of P-gp also express COX-2 [122-124]. In each study, inhibition of COX-2 prevented the upregulation of P-gp [119-124].

The same relationship between COX-2 and P-gp has been observed in BBB endothelial cells [125, 126]. Exposing isolated rat, mouse, or human (from surgical resection of the epileptic focus) brain capillaries to glutamate increased P-gp expression, which could be blocked with a selective COX-2 inhibitor [127-129]. Higher P-gp expression was attenuated in a rat seizure model after a general COX inhibitor [128] and after a specific COX-2 inhibitor [129, 130]. Brain penetration of the AEDs phenytoin [130] and phenobarbital [131] increased in rats with recurrent seizures after COX-2 inhibition. However, another study found inhibition of COX-2 with SC-58236 increased adverse effects in a rat seizure model, and advised against the use of this inhibitor for adjunctive therapy in drug-resistant epilepsy [132]. The few times COX-1 was investigated in relation to ABC transporters, it was found that expression levels are the same between parent and P-gp-expressing cells [122], and that inhibition of COX-1 alone did not sensitize P-gp-expressing cells to doxorubicin, as was the case with COX-2 inhibition [133].

2 AIMS

The original goal of this thesis was to develop a PET imaging paradigm to image BCRP activity at the BBB. However, the development of a radioligand failed because of the lack of a BCRP-specific substrate amendable to radiolabeling. Accordingly, the first goal was restricted to a characterization of the actions of the candidate BCRP inhibitor Ko143, as well as the P-gp inhibitor tariquidar, which is critical to the in vivo utility of an eventual BCRP radiotracer. The second goal remained the same: to explore the roles of efflux transporters and neuroinflammation in drug-resistant epilepsy. After the revised overall goals, the specific aims of the thesis were:

1. To assess the specificity of the BCRP inhibitor Ko143 (paper I)
2. To characterize the inhibitory properties of the P-gp inhibitor tariquidar (paper II)
3. To determine if sclerosis has an impact on ABC transporter expression in drug-resistant epilepsy (paper III)
4. To measure the cellular expression of the inflammatory proteins COX-1, COX-2, and TSPO in drug-resistant epilepsy (paper IV)

3 MATERIALS AND METHODS

3.1 IN VITRO STUDIES

3.1.1 Chemicals

3.1.1.1 Radiotracers

[3H]Ko143 and [3H]tariquidar were synthesized by Moravek Biochemicals (Brea, CA) and American Radiolabeled Chemicals (St. Louis, MO), respectively. Both tracers had a radiochemical purity > 95% as indicated by high-performance liquid chromatography.

3.1.1.2 Pharmacological agents

The P-gp inhibitor (2R)-anti-5-{3-[4-(10,11-dichloromethanodibenzo-suber-5-yl)piperazin-1-yl]-2-hydroxypropoxy}quinoline trihydrochloride (DCPQ) was provided by Dr. Victor W. Pike (National Institute of Mental Health, Bethesda, MD). The remaining chemicals and pharmacological agents were purchased commercially.

3.1.2 Cell lines

Human or mouse ABC transporter-expressing (resistant) and parental (control) cell lines were cultured for use in several in vitro assays (Table 1). The resistant cell lines were cultivated via transfection with plasmids containing cDNA of P-gp, BCRP, or MRP1, or through the addition of pharmacological agents added to the media (Table 1) [134-140]. Parental and resistant HEK-293 cells were provided by Susan Bates (National Cancer Institute, Bethesda, MD) and were grown in Eagle's minimum essential medium (EMEM) supplemented with 2 mg/mL G418. LLC-PK1 cells were grown in Medium-199 supplemented with 500 μg/mL G418, except for the LLC-BCRP cells, which were supplemented with 500 μg/mL zeocin. The remaining cell lines were grown in Dulbecco's modified Eagle's medium (DMEM). Culture medium for all cell lines was supplemented with fetal bovine serum (10% for all cells except LLC cells which received 3%), glutamine, and antibiotic [141]. All cell lines were grown at 37 °C in 5% CO_2.

3.1.3 Animals

A cardiac puncture to collect blood was performed using one Sprague-Dawley rat. Animal experiments were performed in accordance with the Guide for Care and Use of Laboratory Animals [142] and were approved by the National Institute of Mental Health Animal Care and Use Committee.

3.1.4 Cytotoxicity assay

Cytotoxicity assays were used to measure the interaction between ABC transporters and drugs thought to inhibit transporter function. The protocol was followed as described by Brimacombe et al. 2009, with the following modifications [143]. Parental and resistant cell lines were seeded at a density of 4,000 cells/well. Serial dilutions of the transporter-specific

Table 1. Cell lines for papers I and II

Cell Line	Cell Type	Expressed ABC Transporter	Drug Supplementation	Paper
HEK-293	Human embryonic kidney	-	-	
HEK G2	Human embryonic kidney	BCRP	-	Paper I
HEK B1	Human embryonic kidney	P-gp	-	
HEK C1	Human embryonic kidney	MRP1	4 µM Etoposide	
MCF-7	Human breast cancer	-	-	Paper I + II
FLV10000	Human breast cancer	BCRP	10 µg/mL Flavopiridol	
MEF 3.8	Mouse embryonic fibroblast	-	-	Paper I + II
MEF M32	Mouse embryonic fibroblast	Mouse BCRP	32 nM Mitoxantrone	
3T3	Mouse embryonic fibroblast	-	-	Paper I + II
C3M	Mouse embryonic fibroblast	Mouse P-gp	1 µg/mL Colchicine	
KB-3-1	Human adenocarcinoma	-	-	Paper II
KB-8-5-11	Human adenocarcinoma	P-gp	250 nM Colchicine	
LLC-PK1	Porcine kidney	-	-	
LLC-MDR1	Porcine kidney	P-gp	-	Paper II
LLC-ABCG2	Porcine kidney	BCRP	-	

cytotoxic drugs for P-gp (paclitaxel), BCRP (mitoxantrone), or MRP1 (doxorubicin) were made in either EMEM or DMEM. The inhibitors Ko143 and tariquidar were added to the wells to assess the ability of these drugs to reverse resistance. Cell viability was measured using either the CellTiter-Glo Luminescent Cell Viability Assay (Promega, Madison, WI), or the MTT assay [143]. The outcome measure was the half-maximal inhibitory concentration (IC_{50}), which indicates the concentration of cytotoxic drug required to decrease cell viability by 50%.

3.1.5 Flow cytometry

The ability of ABC transporter inhibitors to increase accumulation of fluorescent substrates was measured by flow cytometry. Parental and resistant cells were suspended in either EMEM or DMEM at a density of 2.0×10^5 cells/mL, washed in Iscove's modified Dulbecco's medium, and resuspended in media containing the fluorescent substrate plus or minus an inhibitor. After incubation at 37 °C, cells were washed and resuspended in 0.1% bovine serum albumin in phosphate-buffered saline (PBS), and kept on ice until analysis. The samples were read using a FACSCalibur, or an LSR II flow cytometer (BD Biosciences, San Jose, CA).

3.1.6 ATPase assay

The interaction between ABC transporters and substrates or inhibitors can be measured using an ATPase assay. The protocol described in Kannan et al., 2011 was followed [30]. Briefly, crude membranes isolated from Hi-five insect cells, which expressed P-gp or BCRP, were suspended in ATPase assay buffer. The membranes were incubated with 5 mM ATP, varying concentrations of Ko143 or tariquidar, and with or without beryllium fluoride. The hydrolysis of ATP was measured using a spectrophotometer at 880 nm [144, 145].

14

3.1.7 Radioaccumulation assay

Accumulation of [^{3}H]Ko143 and [^{3}H]tariquidar in parental and resistant cells was used to determine the interaction of these radiotracers with the ABC transporters. Cells were seeded at a density of 2.5×10^5 cells/mL in a 24-well plate. Media containing the radiotracer was added to the cells, with and without a transporter-specific inhibitor. Six wells did not receive radiotracer and were used to account for background noise, while an additional three wells were reserved for cell counts to standardize accumulation. After incubation, media was removed and cells were washed in PBS. The cells were then trypsinized for 90 minutes, after which radioactivity was measured in a liquid scintillation counter.

3.1.8 High-performance liquid chromatography

Reverse-phase high-performance liquid chromatography was used to determine the stability of the BCRP inhibitor Ko143 in plasma. Whole blood was collected from a rat via cardiac puncture, from which the plasma was derived after centrifugation. A saturated solution of Ko143 was added to the plasma, with and without the esterase inhibitor NaF. Ko143 was also added to dimethyl sulfoxide (DMSO) as a negative control. Samples were then taken at 5, 10, 15, 30, and 60 minutes, and acetonitrile was used to stop the reaction. The samples were injected onto a X-terra Prep C18 column (7.8×300 mm; Waters, Milford, MA), and eluted at 4 mL/min.

3.1.9 Transepithelial drug transport assay

LLC-PK1 cells were used to determine the efflux activity of P-gp and BCRP. Cells were seeded at a density of 2×10^6 cells/well on transwell polycarbonate filters. [^{3}H]tariquidar was added to the apical or basolateral side of the monolayer, with and without the addition of a P-gp inhibitor (DCPQ) or a BCRP inhibitor (Ko143 or elacridar). At several time points, samples were taken from the side opposite to where the [^{3}H]tariquidar was added, and radioactivity was measured using a liquid scintillation counter. Fold change in the ratio of efflux was calculated by dividing the basolateral to apical transport by the apical to basolateral transport.

3.2 IMMUNOFLUORESCENCE STUDIES

3.2.1 Human tissue

We obtained human brain tissue from patients with mesial temporal lobe epilepsy. Patients were referred to the Clinical Epilepsy Section, National Institute of Neurological Disorders and Stroke, NIH for drug-resistant epilepsy. The study was approved by the NIH Combined Neurosciences Institutional Review Board. All patients signed informed consent. An overview of patient demographics and pathological diagnosis are provided in Table 2. The tissue was formalin fixed, blocked in paraffin, cut into 5 μm sections, and mounted on microscope slides. The tissue from each patient was classified by a trained neuropathologist as either having mesial temporal sclerosis (MTS) or not (non-MTS) based on guidelines established by the International League Against Epilepsy [146].

Table 2. Patient information for immunofluorescence studies

Set	n	Status	Sex	Average age of onset (years)	Duration (years)
A	20	12 MTS	12 Females	13 ± 12.7	20.1 ± 12.4
B	11	4 MTS	5 Females	11.8 ± 10	19 ± 10.2

3.2.2 Immunofluorescence and scanning

Protein levels were measured using immunofluorescence techniques, in which the expression of primary antibodies bound to specific proteins was visualized using fluorescently conjugated secondary antibodies. A BOND-MAX automated stainer (Leica Biosystems, Wetzlar, Germany) was used to prepare the slides for staining. The sections were baked at 60 °C, dewaxed using Bond Dewax Solution (72 °C, Leica Biosystems), and run through a heat-induced epitope retrieval step (100 °C, pH 9.0). Outside of the automated stainer, the slides were washed in PBS, incubated in 0.03% H_2O_2 for 30 minutes, and washed again. Primary antibodies (Table 3) were diluted in primary antibody buffer (0.3% TX-100, 0.1% NaN_3, PBS), and were added to the slides for overnight incubation at 4 °C. The following day, the slides were washed in Tris-buffered saline (TBS, pH 7.4)-Tween 20 and blocked in Tris-NaCl blocking buffer (TNB) (0.1 M Tris-HCl pH 7.5, 0.15 M NaCl, 0.5% blocking reagent, Perkin Elmer, Waltham, MA) for 30 minutes. The secondary antibody (Table 3) diluted in TNB was then applied to the slides and allowed to incubate for 90 minutes, followed by a wash in TBS-Tween 20. For cases in which a horseradish peroxidase (HRP) conjugated secondary was used, the slides were labeled with a cyanine dye diluted in tyramine signal amplification (TSA) reagent (Perkin Elmer).

To remove lipofuscin autofluorescence in the tissue, the slides were stained with Sudan Black B solution (1% w/v in 70% ethanol, Sigma-Aldrich, St. Louis, MO) for 5 minutes. The slides were then washed in 70% ethanol, followed by a PBS wash, and coverslipped using mounting medium containing a DAPI counterstain (ProLong Gold Antifade Mountant with DAPI, ThermoFisher Scientific, Waltham, MA). Unless otherwise noted, all steps were executed at room temperature.

For multiple staining protocols, efforts were made to use antibodies raised in different species. This was not always possible however, and to accommodate multiple antibodies of the same species on one slide, the antibodies were developed with HRP-TSA-cyanine secondaries. The slides underwent a heat-induced epitope retrieval step as previously described, which removed the primary and secondary antibodies and preserved the covalently-bound fluorophore-labeled tyramide. This allowed the addition of a second antibody without the possibility of cross-reactivity with previous antibodies of the same species. Antibodies from Atlas Antibodies (Bromma, Sweden) were validated using multiple methods: paired antibodies, in situ hybridization, western blots, and pre-adsorption assays.

Table 3. Antibody information for papers III and IV

Protein	1° antibody	Species	Dilution	2° antibody	Species	Dilution	Paper
P-gp	Anti-P-gp (HPA002199, Atlas Antibodies, Sweden)	Rabbit	1:200	HRP-Cy5	Swine anti-rabbit	1:200	Paper III
BCRP	Anti-PTGS1 (HPA054719, Atlas Antibodies, Sweden)	Rabbit	1:1200	HRP-Cy5	Swine anti-rabbit	1:200	Paper III
Glut1	Anti-SLC2A1 (HPA0031345, Atlas Antibodies, Sweden)	Rabbit	1:5000	HRP-FITC	Swine anti-rabbit	1:200	Paper III
COX-1	Anti-PTGS1 (HPA002834, Atlas Antibodies, Sweden)	Rabbit	1:250	HRP-Cy3 HRP-Cy5	Swine anti-rabbit	1:200	Paper III + IV
COX-2	Anti-PTGS2 (HPA001335, Atlas Antibodies, Sweden)	Rabbit	1:750	HRP-Cy3 HRP-Cy5	Swine anti-rabbit	1:200	Paper III + IV
TSPO	Anti-PBR (ab109497, Abcam, U.S.A.)	Rabbit	1:200	Alexa Fluor 595 Alexa Fluor 647	Donkey anti-rabbit	1:200	Paper III + IV
GFAP	Anti-GFAP (ab4674, Abcam, U.S.A.)	Chicken	1:1000	Dylight 488	Donkey anti-chicken	1:200	Paper IV
Iba1	Anti-Iba1 (ab5076, Abcam, U.S.A.)	Goat	1:100	Cy3	Donkey anti-goat	1:200	Paper IV
NeuN	Anti-NeuN, Biotinylated (ab204681, Abcam, U.S.A.)	Rabbit	1:1000	ABC-Cy3.5	Swine anti-rabbit	1:200	Paper IV

Images of the slides were acquired using a fluorescent light microscope (Metasystems, Altlußheim, Germany) fitted with at 10x objective. Whole tissue samples on the slides were imaged using an automated scanning system, which works by acquiring multiple field of view images and subsequently stitching the images together (VSlide Slide Scanning Platform, Metasystems). The emission spectra for the fluorescently conjugated secondary antibodies are as follows: Hoeschst (420-485 nm), fluorescein (490-530 nm), Cy3 (550-570 nm), Cy3.5 (580-595 nm), Cy5 (650-670 nm).

3.2.3 In situ hybridization

To measure mRNA expression, a RNAscope v. 2.5 protocol (Advanced Cell Diagnostics, ACD, Newark, CA) was used in conjunction with the BOND-MAX automated stainer. After undergoing the same slide preparation as outlined above, the slides were incubated with an ACD proteinase for 15 minutes at 40 °C, followed by H_2O_2 for 10 minutes. The slides were then incubated with the mRNA probe for two hours at 42 °C. The slides were exposed to a series of ACD amplification solutions (ACD AMP 1 – 4) for 15-30 minutes at 42 °C. TSA-

cyanine secondaries were applied to the slides for 15 minutes at room temperature, which bound to the HRP on the ACD AMP 4 reagent. In between each step, the slides were washed in Bond Wash Solution (Leica Biosystems). The slides were then stained with Sudan Black, coverslipped, and scanned as outlined above.

3.2.4 Image analysis

To quantify the expression of proteins as detected by immunofluorescence and in situ hybridization, positive pixel intensity was measured using macros in ImageJ (NIH, Bethesda, MD) and scripts written in Matlab (Mathworks, Natick, MA).

3.2.4.1 ImageJ

From whole pieces of tissues, $\leq$ 50 500×500 pixel (900 x 900 μm) regions of interest (ROIs) were randomly generated (Figure 6A). Each ROI contained up to five separate channels: UV, fluorescein, Cy3, Cy3.5, and Cy5 (Figure 6B). In some instances, there was bleed through of the fluorophore in the fluorescein channel into the Cy3 channel, and from the Cy3.5 channel into the Cy3 channel. In these cases, the extent of the bleed through was measured, and subtracted from the primary image. This was only performed for non-overlapping cellular markers and thus did not affect quantitation. For the inflammation studies in which the COX-1, COX-2, or TSPO protein was measured in the Cy5 channel, background noise was removed by subtracting the median pixel intensity from each image. Because the majority of the pixels in any given image in the Cy5 channel were background, the median pixel intensity of the image represented the background pixels. The images were then thresholded based on the median background intensity plus two standard deviations.

3.2.4.2 Matlab

Integrated pixel intensity and average pixel density were used as measures of protein concentration (outlined in appendix). To measure protein expression within specific cell types, masks of the cells were generated and overlaid onto the image of the protein. Total pixel intensity of the protein was then measured within the masks, and average pixel density was calculated by taking the total pixel intensity and dividing it by the number of pixels within the mask. To generate the masks, the edges of the cells were detected using the Sobel method and then smoothed to generate a binary mask. The binary mask was then multiplied by the original cell image, which had been thresholded based on the background levels in a similar manner as described above. This final mask was then applied to the protein images to measure protein expression within the masks (Figure 6C). For proteins measured not within a mask, total pixel intensity was measured within the whole ROI, and average pixel density was calculated by taking the total pixel intensity and diving it by the total number of pixels within the ROI.
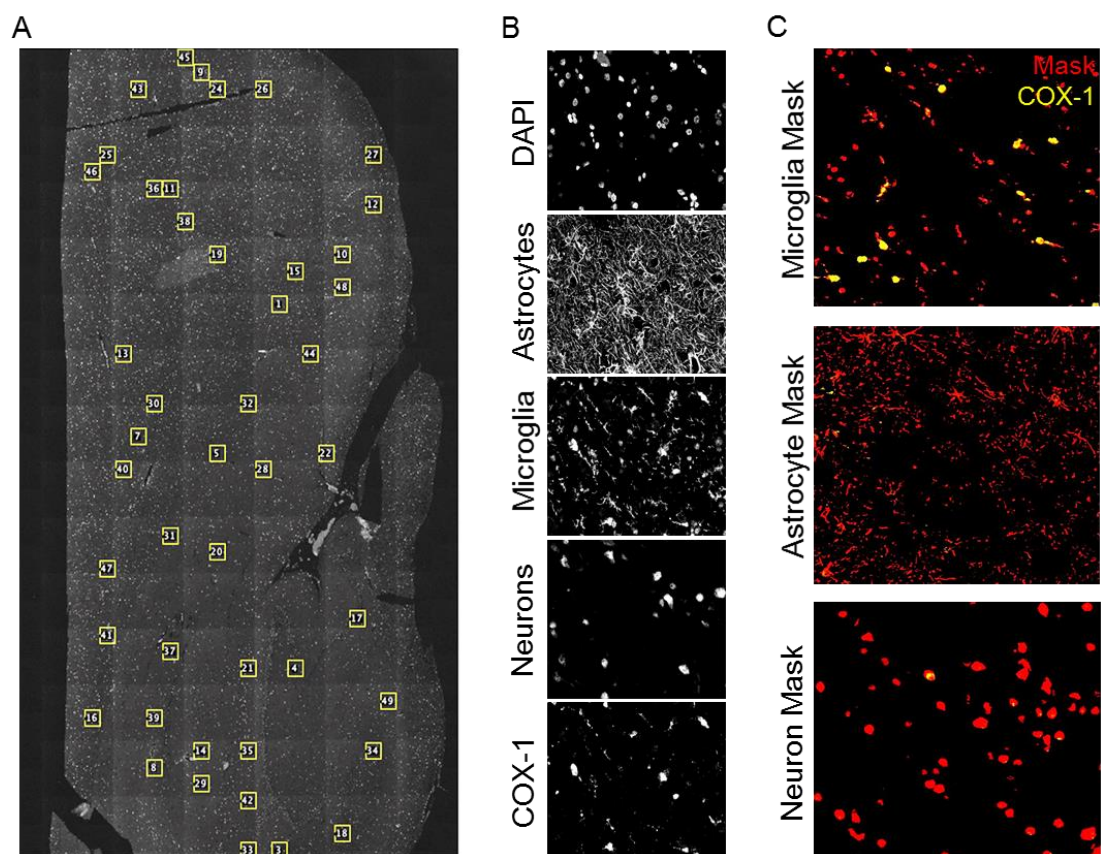
Figure 6. Generation of regions of interest (ROIs) and depictions of cell mask outcomes. (A) From each whole section of tissue, 50 ROIs were randomly generated. (B) Each ROI contained up to five separate channels. As an example, a typical immunofluorescence experiment is shown from paper IV: DAPI in UV, astrocytes (GFAP) in fluorescein, microglia (Iba1) in Cy3, neurons (NeuN) in Cy3.5, and COX-1 in Cy5. (C) Masks of the cells (red) were then overlaid onto the protein image (COX-1 in this example). Yellow indicates positive overlap between the protein and the mask.

3.3 DATA ANALYSIS

3.3.1 In vitro studies

For the cytotoxicity assays, the primary outcome measure was IC_{50}, which indicates the concentration of cytotoxic drug required to reduce cell viability by 50% compared to untreated control cells. Statistical significance was evaluated via Student's *t*-test (unpaired, two-tailed, $\alpha = 0.05$). For the flow cytometry experiments, change in fluorescence was determined via the geometric mean of fluorescence intensity for a total of 10,00 cells per sample. Data were analyzed using Flow Jo software (Tree Star, Ashland, OR).

ATPase activity was measured by comparing the release of inorganic phosphate after incubation with 5 mM ATP before and after the addition of beryllium fluoride. Radioactivity was measured using a scintillation counter, adjusted for cell counts and background noise, and expressed as $fmol/10^6$ cells. Cell counts were obtained from the average of three wells not exposed to radiation, while background noise was obtained from the average of three wells with nonradioactive media.

For the flow cytometry, ATPase, and radioaccumulation assays, statistical significance was determined via a one-way analysis of variance, followed by the Bonferroni post-t test (α = 0.05). Data for all methods are expressed as mean ± SD from three observations, except for the high-performance liquid chromatography experiments in which the data was drawn from one observation.

3.3.2 Immunofluorescence studies

The primary outcome of the immunofluorescence and in situ hybridization studies was the percent integrated density of each target protein. This was calculated by dividing the integrated density of the protein in the whole ROI by the integrated density of protein within the mask. The percent integrated density values from all ROIs (≤ 50) within a piece of tissue were then averaged together. This value was then averaged with all data points from that experiment. The data are expressed as percent mean integrated density ± SD.

Linear regression was used to determine the correlation between ABC transporter and inflammatory protein expression. Wilcoxon rank sum test was used to determine if there were any differences between the MTS and non-MTS groups for each protein. Kruskal-Wallis test followed by the Dunn's multiple comparison test (α = 0.05) was used to determine if there were any significant differences in the expression of each inflammatory protein amongst the different cell types. When combining tissue batches, logistic regression analysis was used to determine if there were any differences between MTS and protein expression, taking into account any batch effect.

4 RESULTS AND DISCUSSION

4.1 ASSESSMENT OF ABC TRANSPORTER INHIBITORS

4.1.1 Ko143 is not selective for BCRP (paper I)

While Ko143 is often utilized as a BCRP inhibitor in vitro, it was not known if Ko143 was specific for BCRP amongst ABC transporters present at the BBB. To this end, we performed multiple in vitro experiments with Ko143 to determine how it interacts with the ABC transporters. The cells used for these experiments expressed BCRP, P-gp, MRP1, or an empty-vector plasmid that acted as the parental cell line (Table 1). The utilization of these cells allowed for measurement of the interaction of Ko143 and tariquidar with each transporter, without the influence of residual transporter expression.

To determine if Ko143 was interacting with a transporter, the extent by which Ko143 inhibited the efflux of transporter-specific substrates was measured. Lower concentrations (nanomolar) of Ko143 reversed resistance in cells expressing human or mouse BCRP to the cytotoxic drug mitoxantrone by ~1.5-fold. Higher concentrations of Ko143 (micromolar) also reversed resistance in cells expressing human or mouse P-gp to paclitaxel by 3-fold and 1.2-fold, respectively, and human MRP1 to doxorubicin by 3.8-fold.

In cells expressing human BCRP, all concentrations of Ko143 tested increased accumulation of mitoxantrone at least 3.5-fold compared to baseline accumulation (Figure 7). The same was found for cells expressing human and mouse P-gp, in which accumulation of rhodamine 123 increased at all concentrations of Ko143 tested by at least 1.5-fold (Figure 7). The most significant increase over baseline was observed in cells expressing human MRP1, in which $10 - 100\ \mu M$ of Ko143 increased calcein-AM accumulation by at least 4-fold (Figure 7).
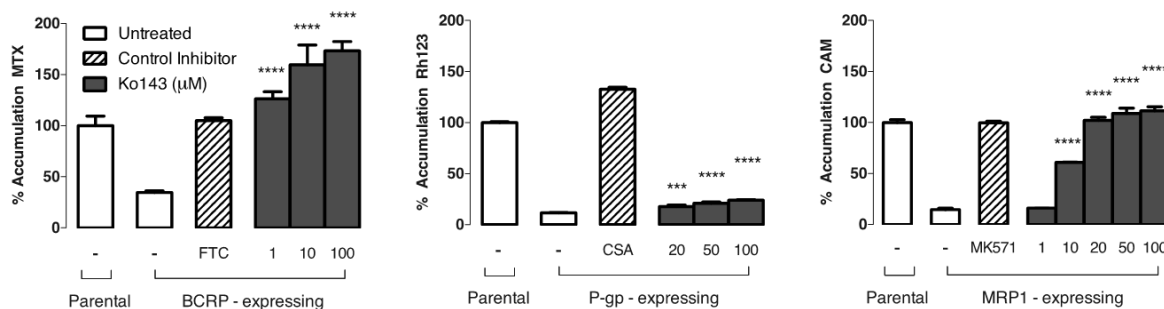

Figure 7. Accumulation of transporter-specific fluorescent substrates in cells expressing BCRP, P-gp, MRP1, or plasmid control before and after administration of the BCRP inhibitor Ko143. Accumulation is low in untreated expressing cells due to efflux of the substrates: mitoxantrone (MTX) for BCRP, rhodamine 123 (rh123) for P-gp, and calcein AM (CAM) for MRP1. Addition of Ko143 however, reverses resistance in all three cells, indicating an interaction between Ko143 and each ABC transporter. This can be compared to the uptake of a transporter-specific inhibitor: fumitremorgin C (FTC) for BCRP, cyclosporin A (CSA) for P-gp, and MK571 for MRP1.
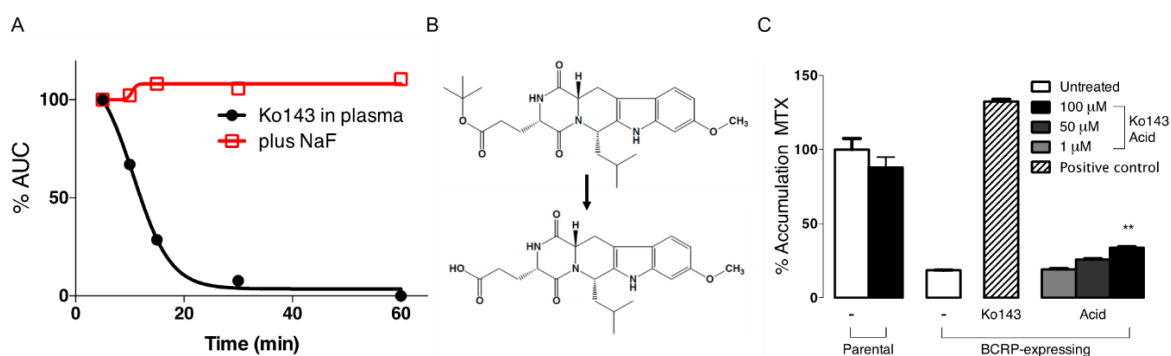
Figure 8. Ko143 is unstable in rat plasma. (A) Ko143 parent compound degrades quickly in rat plasma at room temperature. This is reversed with addition of NaF, implying that the parent compound is hydrolyzed by esterases in plasma. (B) Chemical structure of the Ko143 parent compound (top) and its primary metabolite, Ko143 acid (bottom). (C) Flow cytometry experiment showing that the Ko143 acid has little effect on the accumulation of the fluorescent BCRP substrate mitoxantrone (MTX) in BCRP-expressing cells.

Increased binding of [³H]Ko143 was observed in BCRP-expressing cells compared to parental cells, which was displaced after addition of either non-radioactive Ko143 or fumitremorgin C. There was no difference in the binding in cells expressing either P-gp or MRP1 as compared to parental cells.

Because ABC transporters are ATP-driven efflux pumps, ATPase activity should increase in the presence of a substrate, and decrease in the presence of an inhibitor (there is a basal level of ATPase activity in the absence of substrate). With increasing concentrations of Ko143, ATPase activity decreased in membranes containing BCRP, while it increased in membranes containing P-gp. The same concentration of Ko143 (5 µM) elicited a six-fold decrease in ATPase activity in the BCRP-expressing cells, and a two-fold increase in ATPase stimulation in P-gp-expressing cells.

Since Ko143 has been used to inhibit BCRP in vivo, it is important to understand the stability of Ko143 in plasma, especially given the presence of an ester in the parent compound rendering it susceptible to hydrolysis. At room temperature, Ko143 was unstable in rat plasma and was undetectable at 60 minutes (Figure 8A). Co-incubation with NaF, an esterase inhibitor, inhibited metabolism of Ko143 (Figure 8A). Hydrolysis of the ester group in Ko143 results in a carboxylic acid functional group. We therefore synthesized the Ko143 acid analog (Figure 8B) to determine if the primary metabolic product of Ko143 was also able to inhibit BCRP (or whether it resulted in loss of BCRP inhibitory activity). We found that the acid had a minimal effect on the accumulation of a fluorescent substrate in cells expressing BCRP (Figure 8C), and had no effect on accumulation in cells expressing P-gp, or MRP1. As such, the rapid hydrolysis of Ko143 in blood plasma results in a loss of BCRP inhibitory activity.

The results of this study confirm that Ko143 is a potent inhibitor of both human and mouse BCRP. However, it is clear that at higher in vitro concentrations, Ko143 is not specific for BCRP since it interacts with P-gp and MRP1. In addition, Ko143 was found to be unstable

in rat plasma, although the acid metabolite had no appreciable effect on cellular accumulation. Given that Ko143 is not specific for BCRP and is unstable in plasma, Ko143 should be used with caution for in vitro and in vivo experiments investigating the interaction of substrates with BCRP. An imaging probe could facilitate a study to identify the optimal dose for specific inhibition of BCRP, but not P-gp, so that Ko143 could be used to study BCRP in vivo.

4.1.2 Tariquidar is an inhibitor of P-gp (paper II)

Similar to Ko143, tariquidar is often utilized as an ABC transporter inhibitor. Unlike Ko143, the interactions of tariquidar with P-gp, BCRP, and MRP1 have been defined by Kannan et al. [28]. The authors of this study found tariquidar to be a potent P-gp inhibitor, as well as a substrate of BCRP. Recent reports however, have brought into question the nature by which tariquidar interacts with P-gp, stating that tariquidar is actually a substrate of P-gp [147]. This is significant because this affects whether tariquidar could be used to image P-gp function in PET studies. To address this discrepancy, we measured the interactions of tariquidar with human and mouse P-gp in a similar manner to those described above. A change in the accumulation of transporter-specific substrates after administration of tariquidar was attributed to the influence of tariquidar on the transporter.

Low concentrations (nanomolar) of tariquidar significantly reversed the resistance of cells expressing human and mouse P-gp to paclitaxel by 200- and 20-fold, respectively, compared to baseline. Similar concentrations reversed resistance to the fluorescent P-gp substrate rhodamine 123 in cells expressing human P-gp by 37-fold compared to baseline accumulation. In cells expressing mouse P-gp, 1 μM tariquidar increased cellular accumulation of rhodamine 123 14-fold. Since tariquidar is inherently fluorescent, we could directly measure its intracellular uptake at higher concentrations. In cells expressing P-gp, the cellular accumulation of tariquidar was unchanged after addition of a P-gp inhibitor (Figure 9A). However, in cells expressing BCRP, cellular accumulation of tariquidar increased after inhibition (Figure 9A). Furthermore, 1 μM tariquidar elicited a 50% decrease in ATPase activity in both human and mouse P-gp-expressing membranes (Figure 9B). These experiments indicate that tariquidar is an inhibitor of both human and mouse P-gp since administration of tariquidar leads to increased substrate uptake, and tariquidar itself does not accumulate in P-gp-expressing cells.

ABC transporter inhibitors work by binding to the transporter and thus preventing the transporter from pumping substrates out of the cell. Therefore, while substrates are actively effluxed across a membrane, inhibitors are not. In line with this, we measured no movement of [3H]tariquidar in the basolateral to apical or apical to basolateral direction across membranes expressing P-gp (Figure 9C). Addition of a P-gp inhibitor (1 μM) also had no effect. On the other hand, significant movement of [3H]tariquidar was measured in the basolateral to apical direction across membranes expressing BCRP, consistent with its characterization as a BCRP substrate. Transport in this direction was diminished with the addition of either BCRP inhibitors.

In cellular accumulation studies, [^{3}H]tariquidar binding was 7-fold higher in cells expressing human P-gp than in the parental cells (not lower, as would be anticipated for a substrate of P-gp) (Figure 9D). Addition of non-radioactive tariquidar displaced the [^{3}H]tariquidar binding from the cells (Figure 9D). Similar interactions were observed with [^{3}H]tariquidar and mouse P-gp-expressing cells (Figure 9D). As mentioned above, [^{3}H]Ko143 also displayed similar binding patterns in cells expressing BCRP. Higher accumulation of the tritiated inhibitor is observed because the inhibitor is tightly bound to the transporter. Because the transporter is present in the expressing cell lines, but not the parent cell lines, higher binding of the inhibitors is observed, which is then displaced by competition from another inhibitor. These observations are consistent with another P-gp inhibitor [^{3}H]BIBW22 BS, which showed higher binding to P-gp-expressing cells compared with the parent cells [148].

The results of this study indicate that tariquidar is an inhibitor of P-gp at in vitro concentrations. Any discrepancy in the literature does not appear to be due to species differences, since tariquidar inhibited both human and mouse P-gp. This study could not, however, examine tariquidar interactions with P-gp at picomolar concentrations, which are used in PET imaging with [^{11}C]tariquidar.
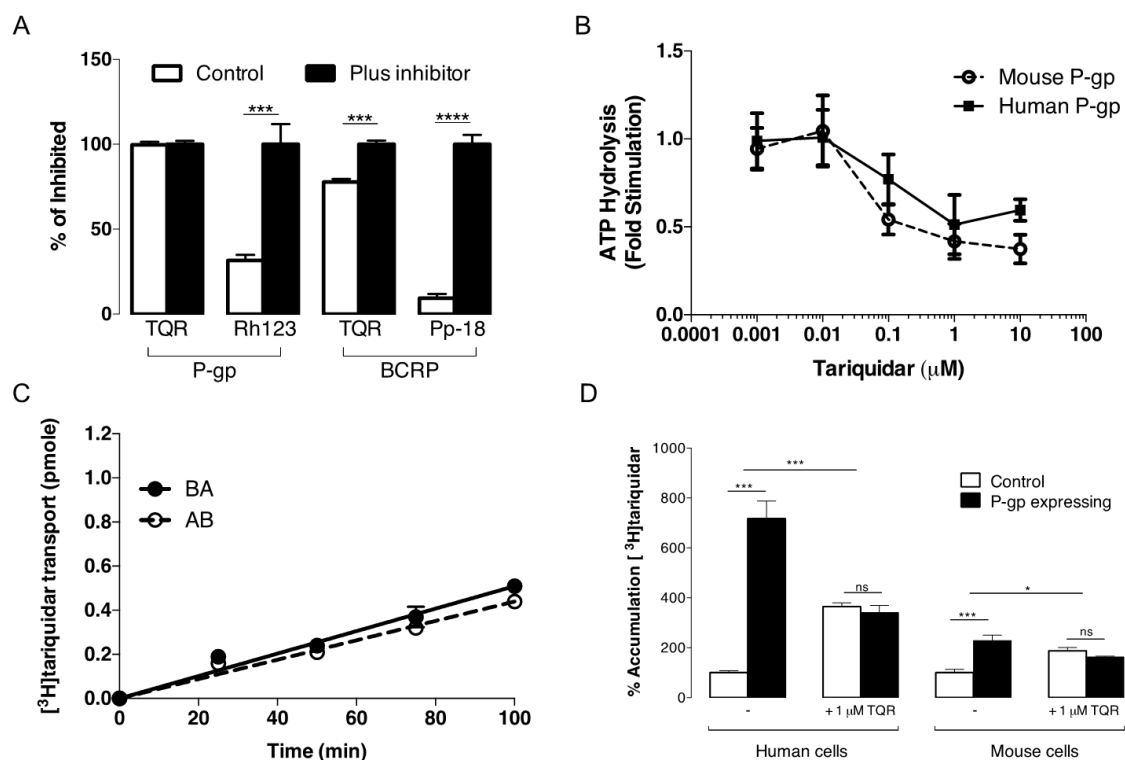

Figure 9. Tariquidar is not a substrate of P-gp based on multiple in vitro assays. (A) No change in intracellular accumulation of tariquidar (which is fluorescent) is observed in P-gp-expressing cells, but can be seen in BCRP-expressing cells. (B) Both mouse and human P-gp show a decrease in ATPase activity with increasing concentrations of tariquidar. If tariquidar were a substrate of P-gp, it would stimulate ATPase activity. (C) Transwell assays show no movement in either direction of [^{3}H]tariquidar across P-gp-expressing membranes. (D) Accumulation of [^{3}H]tariquidar is higher in P-gp-expressing cells than in control cells. This is due to the binding of the inhibitor to the transporter.

4.2 ABC TRANSPORTERS AND INFLAMMATION IN EPILEPSY

4.2.1 ABC transporter expression does not vary with sclerosis (paper III)

The question as to whether ABC transporter expression is increased at the BBB in drug-resistant epilepsy, and whether this increase is the cause of the drug resistance, remains unanswered. Several groups have used immunohistochemistry methods to answer the former, but these studies are plagued by a lack of suitable control tissue given that the type of epilepsy tissue obtained is most often fresh surgical tissue. It is often the case that studies will resort to using post-mortem tissue, or tissue obtained from other types of brain surgeries, as control tissue.

Table 4. Comparison of protein levels between MTS and non-MTS tissue samples

Experiment	MTS (n)	Non-MTS (n)	P-value
P-gp			
1	39.5 (12)	36.8 (8)	0.4081
2	26.5 (12)	26.1 (8)	0.9344
3	40.3 (10)	49.4 (6)	0.0432
BCRP			
1	47.7 (10)	68.1 (7)	0.0512
2	68.4 (12)	81.8 (8)	0.1264
3	35.6 (12)	50.3 (8)	0.0298
4	35.4 (4)	42.2 (7)	0.3932
COX-1			
1	66 (10)	64 (7)	0.8451
2	94.0 (12)	70.6 (8)	0.0165
COX-2			
1	123.1 (12)	119.7 (8)	0.4934
2	92.5 (12)	90.8 (8)	0.7775
TSPO			
1	92.1 (12)	95.9 (8)	0.0566
2	81.7 (10)	84.1 (7)	0.3535
3	74.0 (4)	78.3 (7)	0.7922
Capillary coverage			
1	1.1 (12)	1.1 (8)	0.9577
2	0.80 (12)	1 (8)	0.0919
3	1.2 (10)	1.5 (7)	0.1553
4	1.2 (10)	1.6 (7)	0.2167
5	1.4 (12)	1.9 (8)	0.0303
6	1.1 (12)	1.3 (8)	0.1723

When the epileptic tissue is obtained from the resection surgeries, it can be classified based on the level of MTS observed upon pathological inspection [146]. It was previously shown that the non-MTS tissue was found to be similar in pathology (low levels of sclerosis and gliosis) compared to healthy post-mortem tissue [149]. In light of this, we measured ABC transporter expression in MTS and non-MTS surgical drug-resistant epilepsy tissue samples in the hopes that the non-MTS tissue could be used as a pseudo-control. In addition, we compared the expression of P-gp and BCRP with the expression of the inflammatory proteins COX-1, COX-2, and TSPO.

Previous literature shows an increase in P-gp expression in similar tissue types as compared to post-mortem controls and other surgical tissue [46-55]. However, a strength of the studies described in this thesis is the method used to measure P-gp and BCRP expression. Instead of simply counting positively-stained capillaries, an automated method of detecting and quantifying expression within capillaries (thus normalizing for capillary density) was used (appendix). This allowed for an un-biased quantitative measurement of the density of P-gp and BCRP. As a result of the method used to measure ABC transporter

expression, expression of each protein was measured multiple times across separate experiments. Based on immunofluorescence data, there was no difference in P-gp density between MTS and non-MTS tissue sets (Table 4). The same was true for BCRP, however density in the non-MTS set tended to be higher than in the MTS set (Table 4). No difference was observed in capillary density (as determined by the percent coverage of the glut-1 antibody) between MTS and non-MTS tissue sets (Table 4).

The expression of P-gp and BCRP was also compared to expression of the inflammatory proteins to determine whether ABC transporter expression correlated to inflammation. No significant correlation was observed between P-gp and COX-1, COX-2, or TSPO, as well as between BCRP and COX-1 or COX-2. A positive correlation was observed however, between BCRP density and TSPO density. BCRP density increased in a linear fashion with TSPO density ($P = 0.0003$, r = 0.7213) (Figure 10A). Visual inspection of tissue samples with high and low correlations confirm this relationship (Figure 10B). Intensity plots of the capillaries in Figure 10B show higher gray values (pixel values) for the high-correlation image than for the low-correlation image (Figure 10C). Neither TSPO nor BCRP density was correlated with capillary density. This experiment was repeated upon receiving an additional set of epilepsy tissue (Table 2, Set B), and the same correlation was observed. There has been no mention of a relationship between TSPO and BCRP in the literature, and the meaning behind this observation is unclear. Further experimentation is needed to determine whether there is a causal relationship between increases in TSPO expression and increases in capillary BCRP expression.
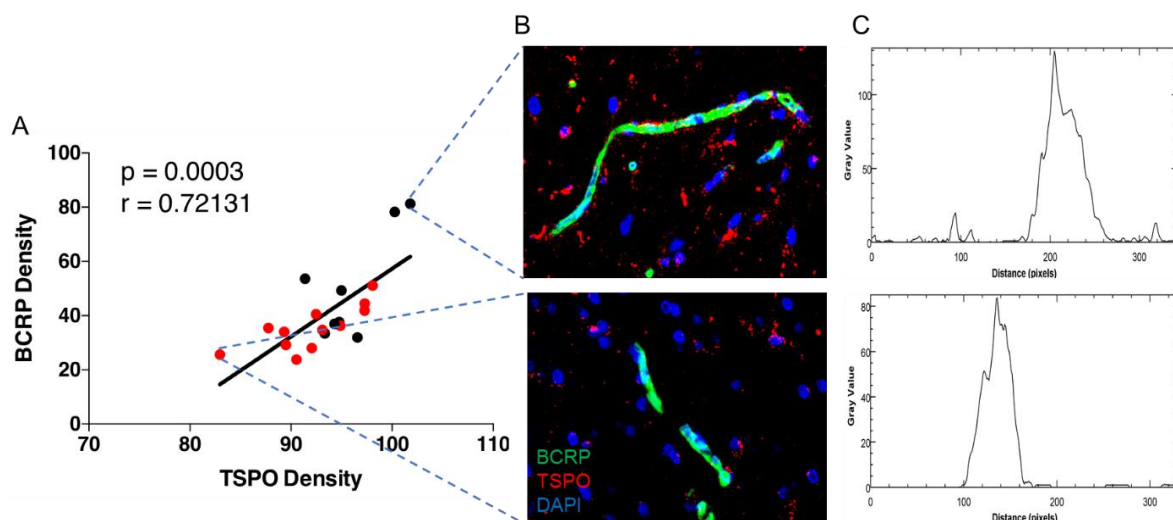

Figure 10. Increases in BCRP density positively correlated with increases in TSPO density. (A) Relationship between BCRP density and TSPO density in tissue set A with MTS (red circles) and non-MTS (black circles) tissue samples. (B) Representative images from a tissue sample with a high correlation between BCRP and TSPO (top) and a low correlation (bottom). (C) Intensity plots of the BCRP capillary staining from the images shown in (B).

No change in the expression of P-gp and BCRP was observed between MTS and non-MTS drug-resistant epilepsy samples. This study was performed based on the idea that non-MTS surgical epilepsy tissue could be used as pseudo-control. Therefore, there are two possible explanations for these results: either there are no differences in the expression of P-gp and BCRP between epilepsy and control tissue samples, or the expression of these transporters is uniform across all types of mesial temporal lobe epilepsy.

4.2.2 Expression of COX-1, COX-2, and TSPO (paper IV)

Inflammation is understood to play a role in some types of epilepsy, but its involvement in mesial temporal lobe epilepsy is unknown. In animal models of epilepsy, expression of COX-1 and COX-2 is upregulated compared to healthy animals, lending further proof that inflammation has a role in epilepsy [150-157]. The cellular localization of COX-1 and COX-2 can in some cases determine the function: COX-1 in platelets produces thromboxane A2 (which enhances coagulation), and COX-2 in vascular endothelium produces prostaglandin I2 (which inhibits coagulation) [158]. Little is known about the cellular localization of COX-1 and COX-2, as well as the inflammation biomarker TSPO, in drug-resistant epilepsy. To address this, we measured the expression of COX-1, COX-2, and TSPO in microglia, astrocytes, and neurons in drug-resistant epilepsy tissue via immunofluorescence and in situ hybridization techniques. The experiments were conducted using both set A and set B of the surgical drug-resistant epilepsy tissue (Table 2).
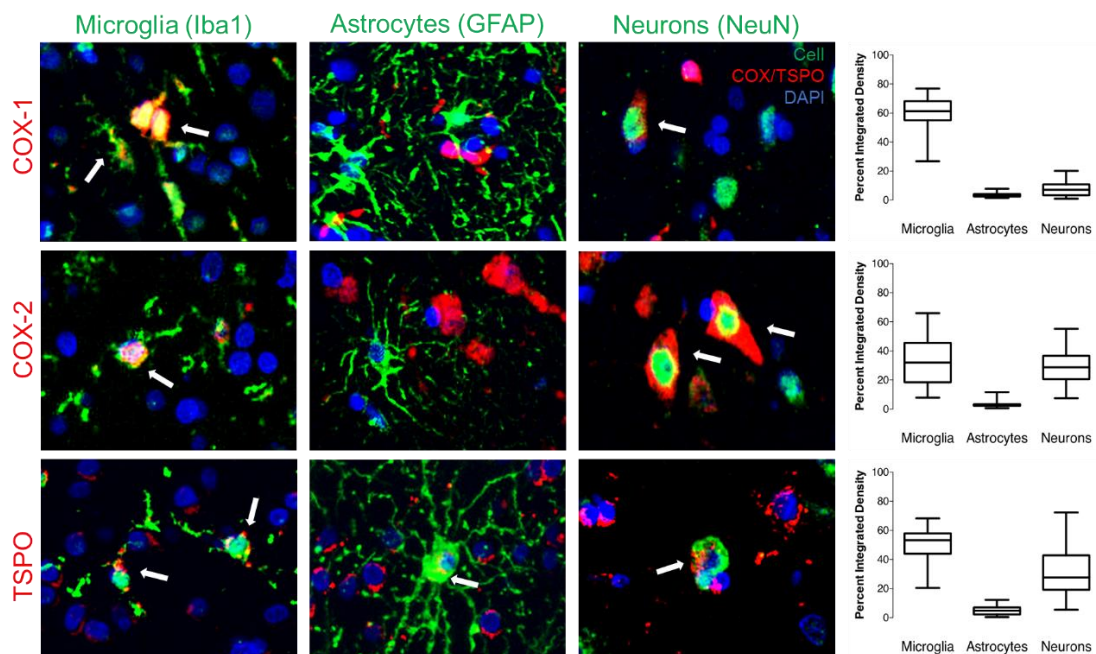

Figure 11. Expression patterns of COX-1, COX-2, and TSPO amongst microglia, astrocytes, and neurons. COX-1 (top row) is primarily expressed in microglia, with minor expression in astrocytes and neurons. COX-2 (middle row) is expressed in both microglia and neurons. TSPO (bottom row) is also expressed in microglia and neurons. In this image, the protein is shown in red, the cell is shown in green, and the DAPI counterstain is shown in blue. White arrows indicate positive overlap between the protein and the cell. Box plots on the right show the quantification of staining patterns across all tissue samples.

To simplify the data as well as to increase power, the immunofluorescence data from the two sets of tissue were pooled and analyzed as a single set. Data is expressed as the percent mean integrated density $\pm$ SD (see Methods). COX-1 (n = 28) levels were significantly higher in microglia (61% $\pm$ 11) than in astrocytes (4% $\pm$ 2, $P < 0.0001$) or neurons (8% $\pm$ 5, $P < 0.0001$) (Figure 11). Expression in neurons was also significantly higher than in astrocytes ($P < 0.05$) (Figure 11). COX-2 (n = 29) expression was significantly higher in microglia (33% $\pm$ 16) and neurons (29% $\pm$ 12) than in astrocytes (3% $\pm$ 2, $P < 0.0001$) (Figure 11). TSPO (n = 31) expression was significantly higher in microglia (50% $\pm$ 12) and neurons (32% $\pm$ 16) than in astrocytes (5% $\pm$ 3, $P < 0.0001$) (Figure 11). In addition, microglia TSPO expression was significantly higher than neuronal TSPO expression ($P < 0.01$) (Figure 11).

No change was observed in the cellular localization of either protein between MTS and non-MTS groups. In addition, total expression (within the whole ROI) for COX-1, COX-2, and TSPO was also unchanged between MTS and non-MTS groups. No change was observed in the density of microglia, astrocytes, and neurons (as determined by the area of the cell mask) between groups. In situ hybridization experiments showed higher mRNA expression in microglia than in astrocytes for COX-1, COX-2, and TSPO. mRNA expression was not measured in neurons because the NeuN antibody was incompatible with the in situ hybridization protocol.

In general, these results coincide with the extant literature: COX-1 is found in microglia and COX-2 is expressed in neurons. However, we found a high expression of COX-2 in microglia, which has not previously been reported. Only two studies have examined the cellular localization of COX-2, and found expression in either astrocytes [159] or neurons [159, 160] in surgical drug-resistant epilepsy tissue. One of these studies did find a difference in COX-2 expression between MTS and non-MTS tissue samples, however the number of tissue samples was low (n = 7) [159].

5 CONCLUSIONS

The first focus of this thesis was to determine the selectivity and specificity of the BCRP inhibitor Ko143, and the P-gp inhibitor tariquidar. We found that although Ko143 is an effective inhibitor of BCRP, it also has an effect on the transport activity of P-gp and MRP1. In addition, we found Ko143 to be unstable in rat plasma, and that the resultant acid has minimal effect on the transporters. We confirmed tariquidar to be a potent inhibitor of both mouse and human P-gp. Tariquidar binds to and inhibits P-gp activity, while it is transported by BCRP.

The second focus of this thesis was to measure the expression of P-gp and BCRP, as well as the inflammatory proteins COX-1, COX-2, and TSPO in surgical brain tissue samples from people with drug-resistant epilepsy. No significant difference in expression of any protein was observed between MTS and non-MTS tissue. A positive linear correlation was found between BCRP expression and TSPO expression. COX-1 was found to be predominately expressed in microglia, while COX-2 and TSPO are expressed in microglia and neurons.

6 FUTURE PERSPECTIVES

Development of a specific substrate radioligand for BCRP. While a PET paradigm exists to image P-gp, this is not the case for BCRP. A specific BCRP substrate amendable to radiolabeling would allow researchers to measure the activity of BCRP in vivo. This is important given the discordant results for BCRP's activity in diseases like drug-resistant epilepsy [56-58]. If BCRP activity is increased in certain diseases, then research can focus on how to bypass its efflux mechanisms at the BBB. This is especially crucial given the finding (addressed in this thesis) that TSPO and BCRP expression are correlated in brain tissue samples from people with drug-resistant epilepsy. PET scans using [^{11}C]PBR28 have shown increased TSPO expression in people with drug-resistant epilepsy [106] so it would be informative to determine if BCRP activity is also increased in the same patients. A BCRP-specific substrate would also allow studies into a range of non-BBB pathologies associated with BCRP including gout and multidrug-resistant cancer.

Determine the relationship between BCRP and TSPO. In brain tissue samples from people with drug-resistant epilepsy, we found a positive linear correlation between BCRP and TSPO expression. This was the only evidence of any relationship between P-gp or BCRP and COX-1, COX-2, or TSPO. Further research is needed to determine if increased density or activity of the cells expressing TSPO and BCRP expression are linked (co-regulated), and the mechanism by which this may occur. In turn, this relationship may provide some insight into ABC transporter expression, and ways in which it can be downregulated in the case of drug resistance.

Determine if there are any differences in COX-2 activity between neurons and microglia. One finding addressed in this thesis is the expression pattern of COX-2. While previous literature has primarily reported neuronal COX-2 in human brain tissue samples [159, 160], we found COX-2 to be expressed in both neurons and microglia. Given that the product of the COX cascade can be dependent on the type of cell it is expressed in [158], further research is warranted to explore if there are any differences in the type of prostanoids produced by COX-2 in neurons versus microglia. If so, it would be interesting to know how neuronal COX-2 expression differs from microglia COX-2 expression under certain disease states.

Development of radioligands to measure COX-1 and COX-2. Measuring inflammation using PET imaging has generally been restricted to TSPO, and while this has been beneficial in many ways, TSPO has its drawbacks. The first is that TSPO is expressed in many cell types, so that increases in signal cannot solely be attributed to microglia alone [161]. Second, astrocytic scarring expresses high levels of TSPO, making TSPO a poor biomarker for acute inflammation [162]. Therefore, radioligands specific for inflammatory proteins are needed to accurately measure acute microglia-specific inflammatory responses. Work is currently underway to implement radioligands specific for COX-1 and COX-2, with the hopes that one or both of these radioligands will fulfill these needs.

7 ACKNOWLEDGEMENTS

To say that this has been a wild ride would be an understatement. If you were to tell me 10 years ago that I would obtain my Ph.D. from one of the top medical schools in Sweden, I would have never in a million years believed you. But here I am! So many people to thank! I will try and keep these short and sweet. Many thanks to the National Institutes of Health (NIH) and Karolinska Institutet (KI) for funding my research, as well as to the following people:

Jan Mulder, my KI supervisor, for teaching me so much about the field of microscopy and immunohistochemistry. Under your tutelage and mentorship, I was able to become a more independent and confident scientist.

Robert Innis, my NIH co-supervisor, for your guidance and mentorship, which made these past four years doable. No matter the situation, you always provided sound advice. I have learned so much from you, especially when it comes to writing and presenting.

Matthew Hall, my NIH co-supervisor, for everything. I wouldn't have been able to do this without you. Your support means the world. Now time for some champagne!

Tomas Hökfelt, my KI co-supervisor, for your devotion to my research, and always taking the time to have discussions with me.

William Theodore, for your help with everything epilepsy related. You were a great resource for knowledge and I very much enjoyed working with you.

Rajesh Narendran, for instilling into me a love of PET. Without your suggestion, I would have never known about or joined this program!

Now for the part that everyone skims just to see if they're mentioned.

My MDR LCB family old and new! *Michael Gottesman*, for adopting me into the LCB family and for our discussions about my research. *Jim Madigan*, for our incredibly entertaining discussions over the years. *Ki Chang*, for your friendship, despite you always stealing my pipette tips ☺. *Janna Moen* and *Jeyan Kumar*, for your friendship both in and out of the lab. *Suresh Ambudkar*, *Suneet Shukla*, and *Andy Fung*, for your scientific help. *Orit Lavi*, *Carol Cardarelli*, *George Leiman*, *Barbara Murphy*, and *Lyn Huff*, for your assistance and support. *Raji Padmanabhan*, for the great Indian food. *Robert Robey*, for your help, advice, and lunch companionship. *Kyle Brimacombe*, for your assistance with my thesis figures.

Tissue profilers! You guys made my time in the Tissue Profiling Lab really awesome and I can't thank you enough for all of the great memories I have of our shenanigans. *Nicholas Mitsios*, for your unwavering support and help with my experiments and beyond. Thank you for all of our discussions, even though most of them were just me complaining about

And of course, to the awesome friends that I have made both at NIH and at KI. *Kristy Pluchino* and *Asia Poprawski*, for the amazing friendship, the lunches, the nights out, the parties (you know which one I'm referring to), the general complaining, and the lots and lots of laughter. I hope you know how much you mean to me, and I look forward to many more parties and laughter in our future. *Adam Thomas*, for the many Game of Thrones discussions over lunch, and *Christina Demaso*, for your shared love of food and cats. I hope you guys have an awesome time in Boston. *Pavitra Kannan*, for your endless amount of help with my research, as well as for your endless support. Also, for your explicitly perfect lab notebook-keeping, which made my first 1.5 years much easier! *Tracy Peters*, for the lunch companionship and support. *Katlyn Parvin*, although we were friends way before graduate school, you were the first to come visit me in Sweden and for that I will forever be grateful. Next time I will know where to go to eat! *Ewoud Ewing*, for sharing your Doctor Who episodes when I was desperate to continue the season, as well as the many lunches at KI and fun times at Vårbergsvägen. *Silke Sohn*, *Paula Kinsoshita*, and *Viktoria Knoflach*, for being the best travel companions and even better friends. I am looking forward to more adventures in the future (although maybe not on cheap cruise ships ☺)! *Julia Remnestål*, for your unwavering friendship and support. You were my first (and best) Swedish friend. You made me feel welcome from the start, and I will forever cherish our fikas and our cat-related discussions. I look forward to many more years of cat-picture swapping, fikas, dinners, and pool-playing. I wish you nothing but the best in your scientific and life pursuits.

To *Dusty* and *Jessica*, for welcoming me to Sweden with open arms. I was very lucky to have family close while in Stockholm.

To my father *Bryan*, for always stressing how important it is to be well-read, and to my mother *Lisa*, for being a close friend and my biggest cheerleader. You guys have pushed me to be the person I am today, and for that I am forever grateful. Without your support and your love, I would never have made it this far. To *Susan*, *Annika*, and *Jim*, for taking the time to visit me in Sweden, and for believing in me. To my brother *Evan*, for all the laughs. I am so proud of you.

To *Muffin*, *Godzilla*, and *Sasha*, for all your love and affection, and for keeping Chris company while I was away.

And lastly, to my husband *Chris*, I cannot stress this enough – none of this would have been possible without you. You are my rock.

8 REFERENCES

[1] Gottesman, M. M., Fojo, T., Bates, S. E., Multidrug resistance in cancer: role of ATP-dependent transporters. *Nat. Rev. Cancer* **2**, 48-58 (2002).

[2] Gottesman, M. M., Mechanisms of cancer drug resistance. *Annu. Rev. Med.* **53**, 615-627 (2002).

[3] Loscher, W., Potschka, H., Drug resistance in brain diseases and the role of drug efflux transporters. *Nat. Rev. Neurosci.* **6**, 591-602 (2005).

[4] Loscher, W., Potschka, H., Role of drug efflux transporters in the brain for drug disposition and treatment of brain diseases. *Prog. Neurobiol.* **76**, 22-76 (2005).

[5] Abbott, N. J., Blood-brain barrier structure and function and the challenges for CNS drug delivery. *J. Inherit Metab. Dis.* **36**, 437-449 (2013).

[6] Pardridge, W. M., Drug transport across the blood-brain barrier. *J. Cereb. Blood Flow Metab.* **32**, 1959-1972 (2012).

[7] Abbott, N. J., Patabendige, A. A., Dolman, D. E., Yusof, S. R., Begley, D. J., Structure and function of the blood-brain barrier. *Neurobiol. Dis.* **37**, 13-25 (2010).

[8] Ueno, M. *et al.*, Transporters in the brain endothelial barrier. *Curr. Med. Chem.* **17**, 1125-1138 (2010).

[9] Waterhouse, R., Determination of lipophilicity and its use as a predictor of blood–brain barrier penetration of molecular imaging agents. *Mol. Imaging Biol.* **5**, 376-389 (2003).

[10] Moitra, K., Dean, M., Evolution of ABC transporters by gene duplication and their role in human disease. *Biol. Chem.* **392**, 29-37 (2011).

[11] Juliano, R. L., Ling, V., A surface glycoprotein modulating drug permeability in chinese hamster ovary cell mutants. *Biochim. Biophys. Acta* **455**, 152-162 (1976).

[12] Ueda, K. *et al.*, The mdr1 gene, responsible for multidrug-resistance, codes for P-glycoprotein. *Biochem. Biophys. Res. Commun.* **141**, 956-962 (1986).

[13] Higgins, C., Callaghan, R., Linton, K. J., Rosenberg, M. F., Ford, R. C., Structure of the multidrug resistance P-glycoprotein. *Cancer Biol.* **8**, (1997).

[14] Sharom, F. J., The P-glycoprotein multidrug transporter. *Essays Biochem.* **50**, 161-178 (2011).

[15] Ambudkar, S. V. *et al.*, Biochemical, cellular, and pharmacological aspects of the multidrug transporter. *Annu. Rev. Pharmacol. Toxicol.* **39**, 361-398 (1999).

[16] Germann, U. A., Pastan, I., Gottesman, M. M., P-glycoproteins: mediators of multidrug resistance. *Cell Biol.* **4**, 63-76 (1993).

[17] Lam, F. C. *et al.*, Beta-amyloid efflux mediated by P-glycoprotein. *J. Neurochem.* **76**, 1121-1128 (2001).

[18] Doyle, L. A. *et al.*, A multidrug resitance transproter from human MCF-7 breast cancer cells. *Proc. Natl. Acad. Sci. U. S. A.* **95**, 15665-15670 (1998).

[19] Staud, F., Pavek, P., Breast cancer resistance protein (BCRP/ABCG2). *Int. J. Biochem. Cell B.* **37**, 720-725 (2005).

[20]   Robey, R. W., Ierano, C., Zhan, Z., Bates, S. E., The challenge of exploiting ABCG2 in the clinic. *Curr. Pharm. Biotechnol.* **12**, 595-608 (2011).

[21]   Meyer zu Schawbesdissen, H. E., Kroemer, H. K., in *Drug Transporters,* M. F. Fromm, R. B. Kim, Eds. (Springer, 2004), chap. 9, pp. 329-351.

[22]   Bruhn, O., Cascorbi, I., Polymorphisms of the drug transporters ABCB1, ABCG2, ABCC2 and ABCC3 and their impact on drug bioavailability and clinical relevance. *Expert Opin. Drug Metab. Toxicol.* **10**, 1337-1354 (2014).

[23]   Matsuo, H. *et al.*, ABCG2/BCRP dysfunction as a major cause of gout. *Nucleos. Nucleot. Nucl.* **30**, 1117-1128 (2011).

[24]   Shaffer, B. C. *et al.*, Drug resistance: still a daunting challenge to the successful treatment of AML. *Drug Resist. Updat.* **15**, 62-69 (2012).

[25]   Tamaki, A., Ierano, C., Szakacs, G., Robey, R. W., Bates, S. E., The controversial role of ABC transporters in clinical oncology. *Essays Biochem.* **50**, 209-232 (2011).

[26]   Martin, C. *et al.*, The molecular interaction of the high affinity reversal agent XR9576 with P-glycoprotein. *Br. J. Pharmacol.* **128**, 403-411 (1999).

[27]   Fox, E., Bates, S. E., Tariquidar (XR9576): a P-glycoprotein drug efflux pump inhibitor. *Drug Profile* **7**, 447-459 (2007).

[28]   Kannan, P. *et al.*, The "specific" P-glycoprotein inhibitor tariquidar is also a substrate and an inhibitor for breast cancer resistance protein (BCRP/ABCG2). *ACS Chem. Neurosci.* **2**, 82-89 (2011).

[29]   Allen, J. D. *et al.*, Potent and specific inhibition of the breast cancer resistance protein multidrug transporter in vitro and in mouse intestine by a novel analogue of fumitremorgin C. *Mol. Cancer Ther.* **1**, 417-425 (2002).

[30]   Kannan, P. *et al.*, Imaging the function of P-glycoprotein with radiotracers: pharmacokinetics and in vivo applications. *Clin. Pharmacol. Ther.* **86**, 368-377 (2009).

[31]   Kannan, P. *et al.*, Factors that limit positron emission tomography imaging of p-glycoprotein density at the blood-brain barrier. *Mol. Pharm.* **10**, 2222-2229 (2013).

[32]   Elsinga, P. H. *et al.*, Carbon-11-labeled daunorubicin and verapamil for probing P-glycoprotein in tumors with PET. *J. Nucl. Med.* **37**, 1571-1575 (1996).

[33]   Kannan, P. *et al.*, N-desmethyl-loperamide is selective for P-glycoprotein among three ATP-binding cassette transporters at the blood-brain barrier. *Drug Metab. Dispos.* **38**, 917-922 (2010).

[34]   Piwnica-Worms, D. *et al.*, Functional imaging of multidrug-resistant P-glycoprotein with an organotechnetium complex. *Cancer Res.* **53**, 977-984 (1993).

[35]   Dizdarevic, S., Peters, A. M., Imaging of multidrug resistance in cancer. *Cancer Imaging* **11**, 1-8 (2011).

[36]   Kreisl, W. C. *et al.*, P-glycoprotein function at the blood-brain barrier in humans can be quantified with the substrate radiotracer 11C-N-desmethyl-loperamide. *J. Nucl. Med.* **51**, 559-566 (2010).

[37] Mairinger, S., Erker, T., Müller, M., Langer, O., PET and SPECT radiotracers to assess function and expression of ABC transporters in vivo. *Curr. Drug Metab.* **12**, 774-792 (2011).

[38] Wanek, T., Mairinger, S., Langer, O., Radioligands targeting P-glycoprotein and other drug efflux proteins at the blood-brain barrier. *J. Label. Compd. Radiopharm.* **56**, 68-77 (2013).

[39] Kumata, K. *et al.*, Radiosynthesis of [13N]dantrolene, a positron emission tomography probe for breast cancer resistant protein, using no-carrier-added [13N]ammonia. *Bioorganic Med. Chem.* **20**, 305-310 (2012).

[40] Takada, Y., Ogawa, M., Suzuki, H., Fukumura, T., Radiosynthesis of [2-(11)C-carbonyl]dantrolene using [(11)C]phosgene for PET. *Appl. Radiat. Isot.* **68**, 1715-1720 (2010).

[41] Hosten, B. *et al.*, [11C]befloxatone brain kinetics is not influenced by Bcrp function at the blood-brain barrier: a PET study using Bcrp TGEM knockout rats. *Eur. J. Pharm. Sci.* **50**, 520-525 (2013).

[42] Wanek, T. *et al.*, A novel PET protocol for visualization of breast cancer resistance protein function at the blood-brain barrier. *J. Cereb. Blood Flow Metab.* **32**, 2002-2011 (2012).

[43] Bakhsheshian, J. *et al.*, Bioluminescent imaging of drug efflux at the blood-brain barrier mediated by the transporter ABCG2. *Proc. Natl. Acad. Sci. U. S. A.* **110**, 20801-20806 (2013).

[44] Kwan, P., Schachter, S. C., Brodie, M. J., Drug-resistant epilepsy. *N. Engl. J. Med.* **365**, 919-926 (2011).

[45] Engel, J., Approaches to refractory epilepsy. *Ann. Indian Acad. Neurol.* **17**, 12-17 (2014).

[46] Aronica, E. *et al.*, Expression and cellular distribution of multidrug resistance-related proteins in the hippocampus of patients with mesial temporal lobe epilepsy. *Epilepsia* **45**, 441-451 (2004).

[47] Dombrowski, S. M. *et al.*, Overexpression of multiple drug resistance genes in endothelial cells from patients with refractory epilepsy. *Epilepsia* **42**, 1501-1506 (2001).

[48] Kubota, H. *et al.*, Distribution and functional activity of P-glycoprotein and multidrug resistance-associated proteins in human brain microvascular endothelial cells in hippocampal sclerosis. *Epilepsy Res.* **68**, 213-228 (2006).

[49] Li, Y. *et al.*, Expression of HIF-1alpha and MDR1/P-glycoprotein in refractory mesial temporal lobe epilepsy patients and pharmacoresistant temporal lobe epilepsy rat model kindled by coriaria lactone. *Neurol. Sci.* **35**, 1203-1208 (2014).

[50] Marchi, N. *et al.*, Significance of MDR1 and multiple drug resistance in refractory human epileptic brain. *BMC Med.* **2**, 37 (2004).

[51] Sisodiya, S. M., Lin, W.-R., Harding, B. N., Squier, M. V., Thom, M., Drug resistance in epilepsy: expression of drug resistance proteins in common causes of refractory epilepsy. *Brain* **125**, 22-31 (2002).

[52] Tishler, D. M. *et al.*, MDR1 gene expression in brain of patients with medically intractable eplipesy. *Epilepsia* **369**, 1-6 (1995).

[53] Ak, H. *et al.*, Expression and cellular distribution of multidrug resistance-related proteins in patients with focal cortical dysplasia. *Seizure* **16**, 493-503 (2007).

[54] Aronica, E. *et al.*, Expression and cellular distribution of multidrug transporter proteins in two major causes of medically intractable epilepsy: focal cortical dysplasia and glioneuronal tumors. *Neuroscience* **118**, 417-429 (2003).

[55] Lazarowski, A. *et al.*, Multidrug resistance proteins in tuberous sclerosis and refractory epilepsy. *Pediatr. Neurol.* **30**, 102-106 (2004).

[56] Sisodiya, S. M. *et al.*, Major vault protein, a marker of drug resistance, is upregulated in refractory epilepsy. *Epilepsia* **44**, 1388-1396 (2003).

[57] Aronica, E. *et al.*, Localization of breast cancer resistance protein (BCRP) in microvessel endothelium of human control and epileptic brain. *Epilepsia* **46**, 849-857 (2005).

[58] Salvamoser, J. D. *et al.*, Glutamate-mediated down-regulation of the multidrug-resistance protein BCRP/ABCG2 in porcine and human brain capillaries. *Mol. Pharm.* **12**, 2049-2060 (2015).

[59] Zhang, C., Kwan, P., Zuo, Z., Baum, L., The transport of antiepileptic drugs by P-glycoprotein. *Adv. Drug Deliv. Rev.* **64**, 930-942 (2012).

[60] Cerveny, L., Pavek, P., Malakova, J., Staud, F., Fendrich, Z., Lack of interactions between Breast Cancer Resistance Protein (BCRP/ABCG2) and selected antiepileptic agents. *Epilepsia* **47**, 461-468 (2006).

[61] Nakanishi, T., Ross, D. D., Breast cancer resistance protein (BCRP/ABCG2): its role in multidrug resistance and regulation of its gene expression. *Chin. J. Cancer* **31**, 73-99 (2012).

[62] Asadi-Pooya, A. A., Razavizadegan, S. M., Abdi-Ardekani, A., Sperling, M. R., Adjunctive use of verapamil in patients with refractory temporal lobe epilepsy: a pilot study. *Epilepsy Behav.* **29**, 150-154 (2013).

[63] Iannetti, P., Parisi, P., Spalice, A., Ruggieri, M., Zara, F., Addition of verapamil in the treatment of severe myoclonic epilepsy in infancy. *Epilepsy Res.* **85**, 89-95 (2009).

[64] Nicita, F. *et al.*, Efficacy of verapamil as an adjunctive treatment in children with drug-resistant epilepsy: a pilot study. *Seizure* **23**, 36-40 (2014).

[65] Borlot, F. *et al.*, A pilot double-blind trial using verapamil as adjuvant therapy for refractory seizures. *Epilepsy Res.* **108**, 1642-1651 (2014).

[66] Bartmann, H. *et al.*, Imaging of P-glycoprotein-mediated pharmacoresistance in the hippocampus: proof-of-concept in a chronic rat model of temporal lobe epilepsy. *Epilepsia* **51**, 1780-1790 (2010).

[67] Syvanen, S. *et al.*, (R)-[11C]verapamil PET studies to assess changes in P-glycoprotein expression and functionality in rat blood-brain barrier after exposure to kainate-induced status epilepticus. *BMC Med. Imaging* **11**, 1-16 (2011).

[68] Syvanen, S. *et al.*, [11C]quinidine and [11C]laniquidar PET imaging in a chronic rodent epilepsy model: impact of epilepsy and drug-responsiveness. *Nucl. Med. Biol.* **40**, 764-775 (2013).

[69] Langer, O. *et al.*, Pharmacoresistance in epilepsy: a pilot PET study with the P-glycoprotein substrate R-[(11)C]verapamil. *Epilepsia* **48**, 1774-1784 (2007).

[70] Feldmann, M. *et al.*, P-glycoprotein expression and function in patients with temporal lobe epilepsy: a case-control study. *Lancet Neurol.* **12**, 777-785 (2013).

[71] Miller, D. S., Regulation of P-glycoprotein and other ABC drug transporters at the blood-brain barrier. *Trends Pharmacol. Sci.* **31**, 246-254 (2010).

[72] Vezzani, A., Aronica, E., Mazarati, A., Pittman, Q. J., Epilepsy and brain inflammation. *Exp. Neurol.* **244**, 11-21 (2013).

[73] Blokzijl, H. *et al.*, Decreased P-glycoprotein (P-gp/MDR1) expression in inflamed human intestinal epithelium is independent of PXR protein levels. *Inflamm. Bowel Dis.* **13**, 710-720 (2007).

[74] Englund, G. *et al.*, Efflux transporters in ulcerative colitis: decreased expression of BCRP (ABCG2) and Pgp (ABCB1). *Inflamm. Bowel Dis.* **13**, 291-297 (2007).

[75] Buyse, M., Radeva, G., Bado, A., Farinotti, R., Intestinal inflammation induces adaptation of P-glycoprotein expression and activity. *Biochem. Pharmacol.* **69**, 1745-1754 (2005).

[76] Iizasa, H. *et al.*, Altered expression and function of P-glycoprotein in dextran sodium sulfate-induced colitis in mice. *J. Pharm. Sci.* **92**, 569-576 (2003).

[77] Kalitsky-Szirtes, J., Shayeganpour, A., Brocks, D. R., Piquette-Miller, M., Suppression of drug-metabolizing enzymes and efflux transporters in the intestine of endotoxin-treated rats. *Drug Metab. Dispos.* **32**, 20-27 (2004).

[78] Saclarides, T. J. *et al.*, Variable expression of P-glycoprotein in normal, inflamed, and dysplastic areas of ulcerative colitis. *Dis. Colon Rectum* **35**, 747-752 (1992).

[79] Fakhoury, M., Lecordier, J., Medard, Y., Peuchmaur, M., Jacqz-Aigrain, E., Impact of inflammation on the duodenal mRNA expression of CYP3A and P-glycoprotein in children with Crohn's disease. *Inflamm. Bowel Dis.* **12**, 745-749 (2006).

[80] Pellequer, Y., Weissenborn, V., Lamprecht, A., Decreased drug penetration in inflamed tissue related to changed mucosal metabolism in experimental colitis. *J. Pharm. Sci.* **96**, 2145-2153 (2007).

[81] Bertilsson, P. M., Olsson, P., Magnusson, K.-E., Cytokines influence mRNA expression of cytochrome P450 3A4 and MDR1 in intestinal cells. *J. Pharm. Sci.* **90**, 638-646 (2001).

[82] Kawauchi, S. *et al.*, Intestinal and hepatic expression of cytochrome P450s and mdr1a in rats with indomethacin-induced small intestinal ulcers. *Int. J. Med. Sci.* **11**, 1208-1217 (2014).

[83] Kawase, A. *et al.*, Distinct alterations in ATP-binding cassette transporter expression in liver, kidney, small intestine, and brain in adjuvant-induced arthritic rats. *J. Pharm. Sci.* **103**, 2556-2564 (2014).

[84] Goralski, K. B., Hartmann, G., Piquette-Miller, M., Renton, K. W., Downregulation of mdr1a expression in the brain and liver during CNS inflammation alters the in vivo disposition of digoxin. *Br. J. Pharmacol.* **139**, 35-48 (2003).

[85] Hartmann, G., Kim, H., Piquette-Miller, M., Regulation of the hepatic multidrug resistance gene expression by endotoxin and inflammatory cytokines in mice. *Int. Immunopharmacol.* **1**, 189-199 (2001).

[86] Hartmann, G., Vassileva, V., Piquette-Miller, M., Impact of endotoxin-induced changes in P-glycoprotein expression on disposition of doxorubicin in mice. *Drug Metab. Dispos.* **33**, 820-828 (2005).

[87] Piquette-Miller, M., Pak, A., Kim, H., Anari, R., Shahzamani, A., Decreased expression and activity of P-glycoprotein in rat liver during acute inflammation. *Pharm. Res.* **15**, 706-711 (1998).

[88] Wang, J.-H., Scollard, D. A., Teng, S., Reilly, R. M., Piquette-Miller, M., Detection of P-glycoprotein activity in endotoxemic rats by 99mTc-sestamibi imaging. *J. Nucl. Med.* **46**, 1537-1545 (2005).

[89] Sukhai, M., Yong, A., Kalitsky, J., Piquette-Miller, M., Inflammation and interleukin-6 mediate reductions in the hepatic expression and transcription of the mdr1a and mdr1b Genes. *Mol. Cell Biol. Res. Commun.* **4**, 248-256 (2000).

[90] Lee, G., Piquette-Miller, M., Influence of IL-6 on MDR and MRP-mediated multidrug resistance in human hepatoma cells. *Can. J. Physiol. Pharmacol.* **79**, 876-884 (2001).

[91] Lee, G., Piquette-Miller, M., Cytokines alter the expression and activity of the multidrug resistance transporters in human hepatoma cell lines; analysis using RT-PCR and cDNA microarrays. *J. Pharm. Sci.* **92**, 2152-2163 (2003).

[92] Sukhai, M., Yong, A., Piquette-Miller, M., Decreased expression of P-glycoprotein in interleukin-1B and interleukin-6 treated rat hepatocytes. *Inflamm. Res.* **50**, 362-370 (2001).

[93] Zollner, G. *et al.*, Hepatobiliary transporter expression in percutaneous liver biopsies of patients with cholestatic liver diseases. *Hepatology* **33**, 633-646 (2001).

[94] Fernandez, C., Buyse, M., German-Fattal, M., Gimenez, F., Influence of the pro-inflammatory cytokines on P-glycoprotein expression and functionality. *J. Pharm. Pharm. Sci.* **7**, 359-371 (2004).

[95] Tan, K. H., Purcell, W. M., Heales, S. J., McLeod, J. D., Hurst, R. D., Evaluation of the role of P-glycoprotein in inflammation induced blood-brain barrier damage. *Neuroreport* **13**, 2593-2597 (2002).

[96] Carvey, P. M. *et al.*, 6-Hydroxydopamine-induced alterations in blood-brain barrier permeability. *Eur. J. Neurosci.* **22**, 1158-1168 (2005).

[97] Bauer, B., Hartz, A. M., Miller, D. S., Tumor necrosis factor alpha and endothelin-1 increase P-glycoprotein expression and transport activity at the blood-brain barrier. *Mol. Pharmacol.* **71**, 667-675 (2007).

[98] Poller, B., Drewe, J., Krahenbuhl, S., Huwyler, J., Gutmann, H., Regulation of BCRP (ABCG2) and P-glycoprotein (ABCB1) by cytokines in a model of the human blood-brain barrier. *Cell Mol. Neurobiol.* **30**, 63-70 (2010).

[99] Ronaldson, P. T., Bendayan, R., HIV-1 viral envelope glycoprotein gp120 triggers an inflammatory response in cultured rat astrocytes and regulates the functional expression of P-glycoprotein. *Mol. Pharmacol.* **70**, 1087-1098 (2006).

[100] von Wedel-Parlow, M., Wolte, P., Galla, H. J., Regulation of major efflux transporters under inflammatory conditions at the blood-brain barrier in vitro. *J. Neurochem.* **111**, 111-118 (2009).

[101] Yu, C. *et al.*, Neuroinflammation activates Mdr1b efflux transport through NFkB: promoter analysis in BBB endothelia. *Cell Physiol. Biochem.* **22**, 745-756 (2008).

[102] Harati, R., Villégier, A.-S., Banks, W. A., Mabondzo, A., Susceptibility of juvenile and adult blood-brain barrier to endothelin-1: regulation of P-glycoprotein and breast cancer resistance protein expression and transport activity. *J. Neuroinflammation* **9**, (2012).

[103] Hartz, A. M., Bauer, B., Block, M. L., Hong, J. S., Miller, D. S., Diesel exhaust particles induce oxidative stress, proinflammatory signaling, and P-glycoprotein up-regulation at the blood-brain barrier. *FASEB J.* **22**, 2723-2733 (2008).

[104] Gibson, C. J., Hossain, M. M., Richardson, J. R., Aleksunes, L. M., Inflammatory regulation of ATP binding cassette efflux transporter expression and function in microglia. *J. Pharmacol. Exp. Ther.* **343**, 650-660 (2012).

[105] Papadopoulos, V. *et al.*, Translocator protein (18kDa): new nomenclature for the peripheral-type benzodiazepine receptor based on its structure and molecular function. *Trends Pharmacol. Sci.* **27**, 402-409 (2006).

[106] Hirvonen, J. *et al.*, Increased in vivo expression of an inflammatory marker in temporal lobe epilepsy. *J. Nucl. Med.* **53**, 234-240 (2012).

[107] Chen, M. K., Guilarte, T. R., Translocator protein 18 kDa (TSPO): molecular sensor of brain injury and repair. *Pharmacol. Ther.* **118**, 1-17 (2008).

[108] Cosenza-Nashat, M. *et al.*, Expression of the translocator protein of 18 kDa by microglia, macrophages and astrocytes based on immunohistochemical localization in abnormal human brain. *Neuropathol. Appl. Neurobiol.* **35**, 306-328 (2009).

[109] Dedeurwaerdere, S. *et al.*, PET imaging of brain inflammation during early epileptogenesis in a rat model of temporal lobe epilepsy. *Eur. J. Nucl. Med. Mol. I.* **2**, 1-13 (2012).

[110] Harhausen, D. *et al.*, Specific imaging of inflammation with the 18 kDa translocator protein ligand DPA-714 in animal models of epilepsy and stroke. *PLOS One* **8**, e69529 (2013).

[111] Bogdanovic, R. M. *et al.*, (R)-[11C]PK11195 brain uptake as a biomarker of inflammation and antiepileptic drug resistance: evaluation in a rat epilepsy model. *Neuropharmacology* **85**, 104-112 (2014).

[112] Gershen, L. D. *et al.*, Neuroinflammation in temporal lobe epilepsy measured using positron emission tomographic imaging of translocator protein. *JAMA Neurol.* **72**, 882-888 (2015).

[113] Aid, S., Bosetti, F., Targeting cyclooxygenases-1 and -2 in neuroinflammation: therapeutic implications. *Biochimie* **93**, 46-51 (2011).

[114] Depboylu, C., Weihe, E., Eiden, L. E., COX1 and COX2 expression in non-neuronal cellular compartments of the rhesus macaque brain during lentiviral infection. *Neurobiol. Dis.* **42**, 108-115 (2011).

[115] Choi, S. H., Aid, S., Bosetti, F., The distinct roles of cyclooxygenase-1 and -2 in neuroinflammation: implications for translational research. *Trends Pharmacol. Sci.* **30**, 174-181 (2009).

[116] Surowiak, P. *et al.*, Relationship between the expression of cyclooxygenase 2 and MDR1/P-glycoprotein in invasive breast cancers and their prognostic significance. *Breast Cancer Res.* **7**, R862-870 (2005).

[117] Raspollini, M. R., Amunni, G., Villanucci, A., Boddi, V., Taddei, G. L., Increased cyclooxygenase-2 (COX-2) and P-glycoprotein-170 (MDR1) expression is associated with chemotherapy resistance and poor prognosis. Analysis in ovarian carinoma patients with low and high survival. *Int. J. Gynecol. Cancer* **15**, 255-260 (2005).

[118] Surowiak, P. *et al.*, Significance of cyclooxygenase 2 and MDR1/P-glycoprotein coexpression in ovarian cancers. *Cancer Lett.* **235**, 272-280 (2006).

[119] Patel, V. A., Dunn, M. J., Sorokin, A., Regulation of MDR-1 (P-glycoprotein) by cyclooxygenase-2. *J. Biol. Chem.* **277**, 38915-38920 (2002).

[120] Ziemann, C., Schafer, D., Rudell, G., Kahl, G. F., Hirsch-Ernst, K. I., The cyclooxygenase system participates in functional mdr1b overexpression in primary rat hepatocyte cultures. *Hepatology* **35**, 579-588 (2002).

[121] Zrieki, A., Farinotti, R., Buyse, M., Cyclooxygenase-2 inhibitors prevent trinitrobenzene sulfonic acid-induced P-glycoprotein up-regulation in vitro and in vivo. *Eur. J. Pharmacol.* **636**, 189-197 (2010).

[122] Fantappie, O. *et al.*, The MDR phenotype is associated with the expression of COX-2 and iNOS in a human hepatocellular carcinoma cell line. *Hepatology* **35**, 843-852 (2002).

[123] Ratnasinghe, D. *et al.*, Cyclooxygenase-2, P-glycoprotein-170 and drug resistance; is chemoprevention against multidrug resistance possible? *Anticancer Res.* **21**, 2141-2148 (2001).

[124] Zatelli, M. C. *et al.*, Cyclooxygenase-2 inhibitors reverse chemoresistance phenotype in medullary thyroid carcinoma by a permeability glycoprotein-mediated mechanism. *J. Clin. Endocrinol. Metab.* **90**, 5754-5760 (2005).

[125] Yousif, S. *et al.*, Induction of P-glycoprotein and Bcrp at the rat blood-brain barrier following a subchronic morphine treatment is mediated through NMDA/COX-2 activation. *J. Neurochem.* **123**, 491-503 (2012).

[126] Zuloaga, K. L., Swift, S. N., Gonzales, R. J., Wu, T. J., Handa, R. J., The androgen metabolite, 5alpha-androstane-3beta,17beta-diol, decreases cytokine-induced cyclooxygenase-2, vascular cell adhesion molecule-1 expression, and P-glycoprotein expression in male human brain microvascular endothelial cells. *Endocrinology* **153**, 5949-5960 (2012).

[127] Avemary, J. *et al.*, Dynamic regulation of P-glycoprotein in human brain capillaries. *Mol. Pharm.* **10**, 3333-3341 (2013).

[128] Bauer, B. *et al.*, Seizure-induced up-regulation of P-glycoprotein at the blood-brain barrier through glutamate and cyclooxygenase-2 signaling. *Mol. Pharmacol.* **73**, 1444-1453 (2008).

[129] Zibell, G. *et al.*, Prevention of seizure-induced up-regulation of endothelial P-glycoprotein by COX-2 inhibition. *Neuropharmacology* **56**, 849-855 (2009).

[130] van Vliet, E. A. *et al.*, COX-2 inhibition controls P-glycoprotein expression and promotes brain delivery of phenytoin in chronic epileptic rats. *Neuropharmacology* **58**, 404-412 (2010).

[131] Schlichtiger, J. *et al.*, Celecoxib treatment restores pharmacosensitivity in a rat model of pharmacoresistant epilepsy. *Br. J. Pharmacol.* **160**, 1062-1071 (2010).

[132] Holtman, L., van Vliet, E. A., Edelbroek, P. M., Aronica, E., Gorter, J. A., Cox-2 inhibition can lead to adverse effects in a rat model for temporal lobe epilepsy. *Epilepsy Res.* **91**, 49-56 (2010).

[133] Yu, L. *et al.*, Enhancement of doxorubicin cytotoxicity on human esophageal squamous cell carcinoma cells by indomethacin and 4-[5-(4-chlorophenyl)-3-(trifluoromethyl)-1H-pyrazol-1-yl]benzenesulfonamide (SC236) via inhibiting P-glycoprotein activity. *Mol. Pharmacol.* **75**, 1364-1373 (2009).

[134] Bakhsheshian, J. *et al.*, Overlapping substrate and inhibitor specificity of human and murine ABCG2. *Drug Metab. Dispos.* **41**, 1805-1812 (2013).

[135] Müller, M. *et al.*, Evidence for the role of glycosylation in accessibility of the extracellular domains of human MRP1 (ABCC1). *Biochemistry* **41**, 10123-10132 (2002).

[136] Robey, R. W. *et al.*, Mutations at amino-acid 482 in the ABCG2 gene affect substrate and antagonist specificity. *Br. J. Cancer* **89**, 1971-1978 (2003).

[137] Robey, R. W., Lin, B., Qiu, J., Chan, L. L., Bates, S. E., Rapid detection of ABC transporter interaction: potential utility in pharmacology. *J. Pharmacol. Toxicol. Met.* **63**, 217-222 (2011).

[138] Shen, D.-W. *et al.*, Multiple drug-resistant human KB carcinoma cells independently selected for high-level resistance to colchicine, adiamycin, or vinblastine show changes in expression of specific proteins. *J. Biol. Chem.* **261**, 7762-7770 (1986).

[139] Hall, M. D. *et al.*, Synthesis and structure-activity evaluation of isatin-beta-thiosemicarbazones with improved selective activity toward multidrug-resistant cells expressing P-glycoprotein. *J. Med. Chem.* **54**, 5878-5889 (2011).

[140] Robey, R. W. *et al.*, Overexpression of the ATP-binding cassette half-transporter ABCG2 (MXR/BCRP/ABCP1), in flavopiridol-resistant human breast cancer cells. *Clin. Cancer Res.* **7**, 145-152 (2001).

[141] Lee, C. G. L. *et al.*, HIV-1 protease inhibitors are substrates for the MDR1 multidrug transporter. *Biochemistry* **37**, 3594-3601 (1998).

[142] Clark, J. D., Gebhart, G. F., Gonder, J. C., Keeling, M. E., Kohn, D. F., Guide for the Care and Use of Laboratory Animals. *ILAR Journal* **38**, 41-48 (1996).

[143] Brimacombe, K. R. *et al.*, A dual-fluorescence high-throughput cell line system for probing multidrug resistance. *Assay Drug Dev. Technol.* **7**, 233-249 (2009).

[144] Ambudkar, S. V., Drug-stimulatable ATPase activity in crude membranes of human MDR1-transfected mammalian cells. *Methods Enzymol.* **292**, 504-514 (1998).

[145] Shukla, S., Robey, R. W., Bates, S. E., Ambudkar, S. V., The calcium channel blockers, 1,4-dihydropyridines, are substrates of the multidrug resistance-linked ABC drug transporter, ABCG2. *Biochemistry* **45**, 8490-8951 (2006).

[146] Blumcke, I. *et al.*, International consensus classification of hippocampal sclerosis in temporal lobe epilepsy: a Task Force report from the ILAE Commission on Diagnostic Methods. *Epilepsia* **54**, 1315-1329 (2013).

[147] Bankstahl, J. P. *et al.*, Tariquidar and elacridar are dose-dependently transported by P-glycoprotein and Bcrp at the blood-brain barrier: a small-animal positron emission tomography and in vitro study. *Drug Metab. Dispos.* **41**, 754-762 (2013).

[148] Liu, Z. *et al.*, BIBW22 BS, potent multidrug resistance-reversing agent binds directly to p-glycoprotein and accumulates in drug-resistant cells. *Mol. Pharmacol.* **50**, 482-492 (1996).

[149] De Lanerolle, N. C. *et al.*, A retrospective analysis of hippocampal pathology in human temporal lobe epilepsy: evidence for distinctive patient subcategories. *Epilepsia* **44**, 677-687 (2003).

[150] Hashimoto, K. *et al.*, Behavioral changes and expression of heat shock protein hsp-70 mRNA brain-derived neurotrophic factor mRNA, and cyclooxygenase-2 mRNA in rat brain following seizures induced by systemic administration of kainic acid. *Brain Res.* **804**, 212-223 (1998).

[151] Jiang, J. *et al.*, Therapeutic window for cyclooxygenase-2 related anti-inflammatory therapy after status epilepticus. *Neurobiol. Dis.* **76**, 126-136 (2015).

[152] Joseph, S. A. *et al.*, Enhanced cyclooxygenase-2 expression in olfactory-limbic forebrain following kainate-induced seizures. *Neuroscience* **140**, 1051-1065 (2006).

[153] Kim, D. K., Jang, T. J., Cyclooxygenase-2 expression and effect of celecoxib in flurothyl-induced neonatal seizure. *Int. J. Exp. Path.* **87**, 73-78 (2006).

[154] Kunz, T., Oliw, E. H., The selective cyclooxygenase-2 inhibitor rofecoxib reduces kainate-induced cell death in the rat hippocampus. *Eur. J. Neurosci.* **13**, 569-575 (2001).

[155] Okada, K., Yuhi, T., Tsuji, S., Yamashita, U., Cyclooxygenase-2 expression in the hippocampus of genetically epilepsy susceptible El mice was increased after seizure. *Brain Res.* **894**, 332-335 (2001).

[156] Tanaka, S. *et al.*, Stage- and region-specific cyclooxygenase expression and effects of a selective COX-1 inhibitor in the mouse amygdala kindling model. *Neurosci. Res.* **65**, 79-87 (2009).

[157] Tu, B., Bazan, N. G., Hippocampal kindling epileptogenesis upregulates neuronal cyclooxygenase-2 expression in neocortex. *Exp. Neurol.* **179**, 167-175 (2003).

[158] Steffel, J., Luscher, T. F., Ruschitzka, F., Tanner, F. C., Cyclooxygenase-2 inhibition and coagulation. *J. Cardiovasc. Pharmacol.* **47**, 15-20 (2006).

[159] Desjardins, P. *et al.*, Induction of astrocytic cyclooxygenase-2 in epileptic patients with hippocampal sclerosis. *Neurochem. Int.* **42**, 299-303 (2003).

[160] Fiala, M. *et al.*, Chemotactic and mitogenic stimuli of neuronal apoptosis in patients with medically intractable temporal lobe epilepsy. *Pathophysiology* **20**, 59-69 (2013).

[161] Rupprecht, R. *et al.*, Translocator protein (18 kDa) (TSPO) as a therapeutic target for neurological and psychiatric disorders. *Nat. Rev. Drug Discov.* **9**, 971-988 (2010).

[162] Martin, A. *et al.*, Evaluation of the PBR/TSPO radioligand [(18)F]DPA-714 in a rat model of focal cerebral ischemia. *J. Cereb. Blood Flow Metab.* **30**, 230-241 (2010).